Chapter 4 – NON-LINEAR FIBERS

4.1 BACKGROUND AND PREVIOUS WORK

High brightness broadband sources in the 2 µm to 5 µm atmospheric window with good beam quality and small divergence are needed for spectroscopy and metrology as well as defence applications. Optical fibers are the most interesting technology for Supercontinuum (SC) generation because they permit confining the pump laser pulse into a very small area core and thus the laser pulse interacts with a non-linear medium (here the fiber glass) over a long distance with relatively low losses. Now, the majority of SC sources developed are based on silica fibers, for example [1]-[5]. Especially silica photonic crystal fibers are very unique media in which dispersion and non-linear properties can be tailored by a suitable design of their microstructures [6]. However, as a result of multi-photon absorption, spectral broadening in silica glasses is limited to below 3 µm [7], which makes them unsuitable for continuum generation in the Mid-Infrared (MIR) spectral band. Therefore, soft glasses including tellurite [8]-[10], chalcogenide [11]-[13], fluoride [14]-[16], and lead-bismuth-gallate [17] glasses have been adopted for MIR SC generation. Tellurite, fluoride and lead-bismuth-gallate glasses exhibit high optical transparency in the long-wavelength range of up to ~ 5 µm [8],[17],[18], while chalcogenide glasses are transparent even above 7 µm wavelength [19].

There have been several demonstrations of SC generation with soft glass optical fibers [2],[9],[15],[20]-[25]. SC sources using fluorozirconate based fibers have reached watt level powers, but are restricted to wavelengths below 4 µm when using long fibers. The intrinsic fiber loss due to the multi-phonon absorption edge in fluorozirconate-based fibers is the main limitation on the long-wavelength side for SC generation [26]. Emission beyond the multi-phonon absorption edge can be overcome using short lengths of fiber and high pump intensity and has been demonstrated also in telluride [9] and fluoride fibers [15], but requires the use of high peak power laser sources which are sensitive to mechanical vibrations and temperature fluctuations. On the other hand, micron-sized suspended core fibers offer the possibility to adjust the fiber dispersion and enhance the SC generation; however, these small core fibers cannot sustain high average laser powers. Chalcogenide fibers are chemically stable to air humidity and their non-linear responses is about 500 times higher than fluoride glasses [27]-[30], but their damage threshold is lower than fluoride glasses. Usually, the chalcogenide fiber damage threshold is about 10 times lower than for fluoride fiber which is an important issue when multi-watt average power is required at the output of a single-mode fiber. The proper fiber for the conception of a ruggedized multi-watt SC fiber source into the 2 µm to 5 µm atmospheric windows is explored intensively by many research groups and the recent progresses in fiber technologies indicate that such objectives should be reached in a near future.

SC generation in soft glass fibers is a relatively new research domain and the number of research groups dealing with this topic is still very small. Nevertheless, the results already achieved are very impressive and promising regarding practical applications of SC sources. A very important issue for MIR SC sources ($\lambda > 2$ µm) is the efficiency of SC power distribution towards red wavelengths in relation with the wavelength of pump signal. It directly affects their practical usage in such areas as direct infrared countermeasure or infrared spectral fingerprinting. In this section, we review 3 main techniques for mid-infrared SC generation, i.e. in step-index ZBLAN fibers, in step-index chalcogenide fibers, and in Tellurite fibers. Others micro-structured fibers or exotic glasses are not considered here because the achieved output power is generally low, i.e. less than 100 mW in the MIR spectral range. For this review, Table 4-1 points out the main results published in the literature before the NATO SET-170 started in September 2010 with the emphasis on the results having the highest average power and/or the broadest MIR spectrum. On the other hand, Table 4-2 presents the MIR supercontinuum parameters for the most powerful laser sources developed by various groups during the 3-year mandate of the NATO SET-170. By comparing the data of both tables, we clearly see a rapid increase of the MIR supercontinuum bandwidth and its average power during the last few years. It is interesting to note that the members of the NATO SET-170 obtained similar results that the one listed in Table 3-1 for the ZBLAN fibers while it is Dr. Sanghera's group (member of NATO SET-170) that obtained the highest average power and the broadest supercontinuum in chalcogenide fibers [31].

Table 4-1: Parameters of Supercontinuum Fiber-Based Laser Sources Prior to NATO-SET-170.

Fibers	References	Total Average Power	Spectral Width	MIR Power	
				> 2 µm	> 3 µm
Step-Index ZBLAN	[32]	1.3 W	1.95 – 2.55 µm	~ 0.6 W	~ 0.2 W
	[33]	10.5 W	0.8 – 4.2 µm	~ 5 W	~ 1.1 W
Step-Index Chalcogenide	[34]	0.04 W	1.2 – 2.5 µm	~ 0.0001 W	N/A
Tellurite Fiber	[9]	0.09 W	0.8 – 4.8 µm	~ 0.01 W	~ 0.006 W

Table 4-2: Parameters of Supercontinuum Fiber-Based Laser Sources Developed by Various Groups During the Mandate of the NATO-SET-170.

Fibers	References	Total Average Power	Spectral Width	MIR Power	
				> 2 µm	> 3 µm
Step-Index ZBLAN	[35]	3.9 W	0.75 – 4.3 µm	~ 2.5 W	1.3 W
	[23]	2.6 W	1.9 – 4.5 µm	~ 2.5 W	~ 1 W
	[36]	7.1 W	1.9 – 3.9 µm	~ 6.5 W	~ 2.5 W
Step-Index Chalcogenide	[31]	0.56 W	1.9 – 4.8 µm	~ 0.55 W	~ 0.18 W
Tellurite Fiber	[37]	0.1 W	0.9 – 4.2 µm	N/A	N/A

In order to achieve significant spectral broadening, the zero Group Velocity Dispersion (GVD) of the fiber should be close to the center wavelength of the laser pulse used for SC generation, with the laser wavelength slightly shifted towards the anomalous GVD regime. This minimizes the walk-off between the different regions of the generated spectrum, allowing for further spectral broadening [38]. The GVD of a fiber is first determined by its core material and the diameter of the fiber core. Depending of the refractive indexes of the glass used for the fiber, the fiber GVD is very similar to the glass GVD when its core diameter is larger than ~ 10 µm. For smaller core, the waveguide dispersion tends to shift the zero GVD wavelength towards shorter wavelengths. Such tendency explains the development of microstructured core fibers in order to match the zero GVD wavelength of the fiber with the central wavelength of ultrashort and powerful lasers for the generation of supercontinuum.

For all the results presented above in Table 4-1 and Table 4-2, the supercontinuum generation is generally initiated by self-phase modulation and four-wave mixing which induce primarily the spectral broadening before higher order dispersion causes fission of the laser pulse. After the fission of the laser pulse into multiple solitons, the individual solitons redshift by the Raman self-frequency shift effect and emit phase-matched dispersive waves at wavelengths shorter than the zero GVD [39]. All these non-linear effects are intensity dependent, therefore the fiber core diameter, the fiber dispersion, the initial laser pulsewidth and peak power are important parameters that directly impact the supercontinuum efficiency.

From the results presented in Table 4-1 and Table 4-2 there is a very interesting approach to generate SC in a tandem of silica and fluoride fibers which was proposed by Xia et al. [32],[33] – a technique permitting to eliminate the need of using high peak power mode-locked lasers. The SC generation was initiated by the breakup of amplified nanosecond pulses in a piece of conventional silica Single-Mode Fiber (SMF) into a train of soliton-like sub-pulses through Modulation Instability (MI) and then, as a result of Raman scattering, the spectrum was further broadened in a ZBLAN fiber to over ~ 4 μm wavelength. A unique feature of this solution, differencing it from the other approaches mentioned above, is the possibility of boosting the output average power while keeping the spectrum shape and width relatively constant. The group has already presented the linear scaling up of the average output power to 10.5 W with a spectrum of ~ 0.8 μm to 4 μm using erbium and erbium:ytterbium power fiber amplifiers [33] as well as 5.3 W in a continuum extending from ~ 1.9 μm to 4.5 μm when applying an additional amplification stage based of Tm-doped fibers [23].

In the following sections, we present different experimental schemes for supercontinuum generation obtained by the NATO SET-170 Task Group members. In Section 4.2.1 we demonstrate broadband and powerful supercontinuum generation in step-index ZBLAN fiber. Supercontinuum generation in chalcogenide fiber is also presented in Section 4.2.2, and finally, Section 4.2.3 presents recent results on supercontinuum generation in Indium fluoride-based fibers.

4.2 EXPERIMENTAL RESULTS

4.2.1 Supercontinuum Generation in ZBLAN Fibers

4.2.1.1 Three-Octave Spanning Supercontinuum Generated in a Fluoride Fiber Pumped by Er and Er:Yb-Doped and Tm-Doped Fiber Amplifiers

Contributors to this section: Jacek Swiderski[1], Maria Michalska[1]

From: Optics & Laser Technology 52, 75-80 (2013)

In this section we demonstrate broadband 0.9 – 3.6 μm supercontinuum generation with 0.66 W of output power, using a single-mode fluoride (ZBLAN) fiber pumped by 1.55 μm nanosecond pulses amplified in a cascade of fiber amplifiers. Expanding the pump source by adding an additional amplification section based on thulium-doped fibers, the long-wavelength edge of the spectrum was shifted to ~ 4 μm and was limited by intrinsic losses of the used non-linear ZBLAN fiber. For this cases, the average SC power as high as 288 mW was recorded, of which 266 mW (92%), 167 mW (58%) and 60 mW (21%) corresponds to wavelengths longer than 2 μm, 3 μm and 3.6 μm, respectively.

4.2.1.1.1 SC Generation with the Use of 1.55 μm Fiber Amplifier

The SC generator schematic is shown in Figure 4-1. The pump source was arranged as a fiber MOPA system consisting of a seed and a cascade of three fiber amplifiers. The MOPA output was directly spliced to a piece of SMF followed by a single-mode ZBLAN fiber.

[1] Institute of Optoelectronics, Military University of Technology, 2 Kaliskiego Street, 00-908 Warsaw, Poland.

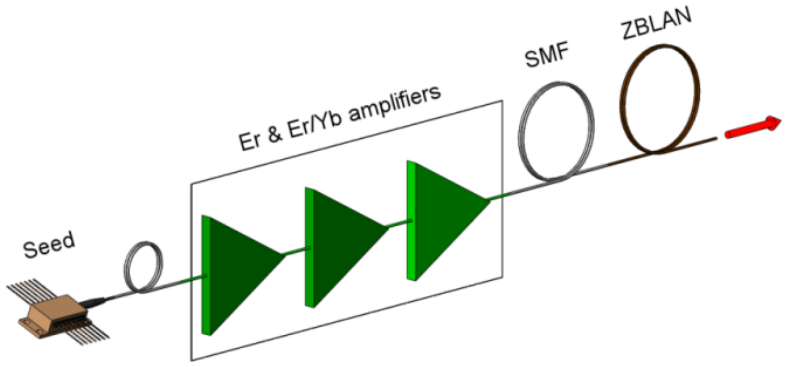

Figure 4-1: Set-Up of SC Source Pumped by a 1.55 µm MOPA.

A 1549.5 nm Distributed Feedback (DFB) laser was used as a seed of ~ 1 ns pulses generated at the Pulse Repetition Frequency (PRF) of 200 kHz. The average output power for this duty cycle was 3 µW, which corresponds to the pulse energy and pulse peak-power of 15 pJ and 15 mW, respectively. Such a pulse train was amplified in a three-stage fiber amplifying cascade, formed by two erbium preamplifiers (EDFAs) and a booster erbium/ytterbium amplifier (EYDFA).The EDFAs utilized single-mode, single-clad erbium-doped fibers with the core diameter of 4 µm and they were pumped by up to 1.5 W of total power at 976 nm wavelength. The booster amplifier was made with the use of 2.4-m long Er:Yb-co-doped double-clad fiber characterized by 6.5 µm / 0.19 NA core and 125 µm / 0.45 NA octagonal clad pumped in counter-propagating scheme (via a multi-mode pump power combiner) by a fiber-coupled laser diode delivering of up to 10 W of continuous power at a wavelength of 976 nm. The power amplifier provided gain of up to 12.5 dB. To block any back reflections, each laser system stage was optically isolated. Also, to eliminate the out-of-band amplified spontaneous emission generated by the active ions, the 100 GHz band-pass filters were used. The entire system provided up to 58.5 dB of total gain. All the SC system components were fusion spliced, thus providing an all-fiber architecture.

The fiber MOPA output (that is 0.5-m long output fiber pigtail of the pump combiner used in the construction of EYDFA) was fusion spliced with a standard SMF-28 having a length of ~ 2.5 m. Finally, the laser radiation coming out of the SMF was launched via bulk optics to a ZBLAN fiber with a ~ 55% efficiency. The 20-m long ZBLAN fiber, with attenuation curve shown in Figure 4-2, had a core/clad diameter of 7/125 µm and a NA of 0.23. The ZDW and cut-off wavelength of this fiber were 1.9 µm and 2.04 µm, respectively.

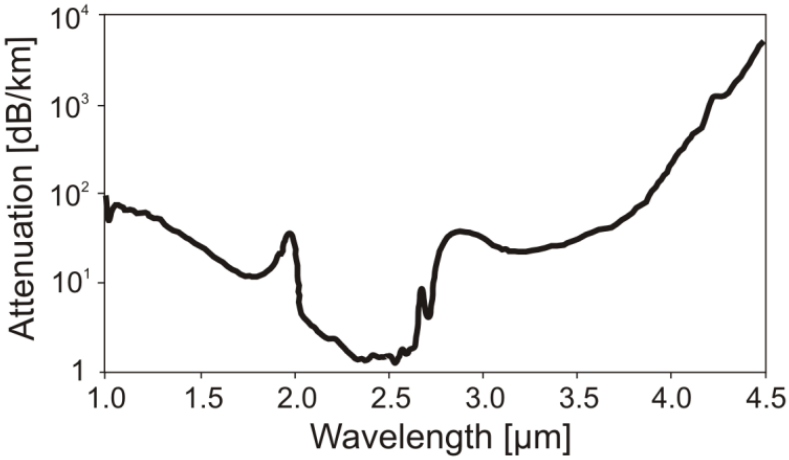

Figure 4-2: Attenuation of the ZBLAN Fiber.

Output SC spectra from 0.6 to 2.4 µm wavelength were measured by using two optical spectrum analyzers whereas the longer wavelengths were recorded with a grating monochromator and a HgCdTe detector. Then the measured spectra were spliced together. The output average SC power was measured by a power meter (Ophir, Laserstar) with thermal sensor (response range of 0.19 to 20 µm).

4.2.1.1.2 SC Generation with the Use of Tm-Doped Fiber Amplifier

The principle scheme of the SC laser source built with the use of Tm^{3+}-Doped Fiber Amplifiers (TDFAs) is shown in Figure 4-3. A significant part of the system is based on the MOPA described in Section 4.2.1.1.1. In this approach, two TDFAs were added.

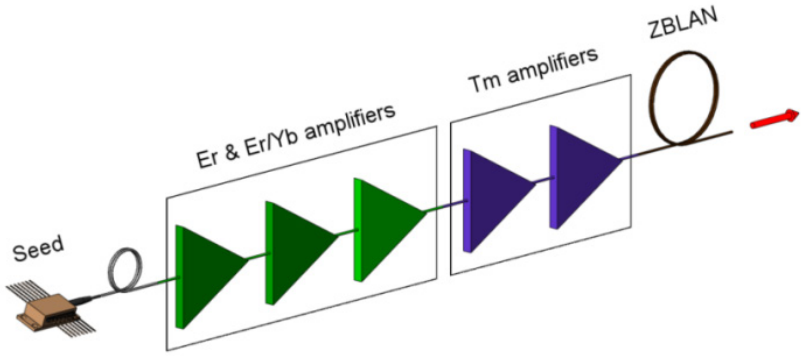

Figure 4-3: Set-Up of SC Source Pumped by Tm-Fiber Amplifiers.

The MOPA fiber output was spliced to a 1-m long single-mode double-clad Tm^{3+}-Doped Fiber (TDF) (dopant concentration, 2 wt. %) with core/clad diameter of 10/130 µm and corresponding NA of 0.15/0.46. It was core-pumped by the 1.55 µm signal coming out of the Er and Er:Yb amplifiers. Then the output from the first TDF was launched into the second 2.5-m long TDF with the same parameters as defined above. It was cladding pumped (in forward configuration) via a (2 x 1) + 1 pump combiner combining two fiber-pigtailed 4.75 W 790-nm pump laser diodes with 105 µm core diameter and 0.22 NA. The fiber end was angle-cleaved to prevent any back reflections. Like in the previous set-up, all the SC system components were fusion spliced to provide an all-fiber format. Finally, the signal amplified and initially broadened in a cascade of TDFAs was launched into the ZBLAN fiber with the use of a telescope allowing for coupling efficiency of ~ 60%. Since fluoride glass has a much lower melting point of about 260°C than silica glass (~ 1200°C), it was not possible to directly fusion splice the two fibers. Both ends of the fluoride fiber as well as the output fiber end of the second TDFA were polished at an angle of 8° to avoid any back reflections.

4.2.1.1.3 SC Generation with the Use of 1.55 µm Fiber Amplifier

The maximum average output power provided by the MOPA system, measured at the SMF output, was 1.56 W. About 0.85 W of this power was coupled into the ZBLAN fiber indicating to ~ 55% launching efficiency. The output SC power as a function of launched pump power is shown in Figure 4-4.

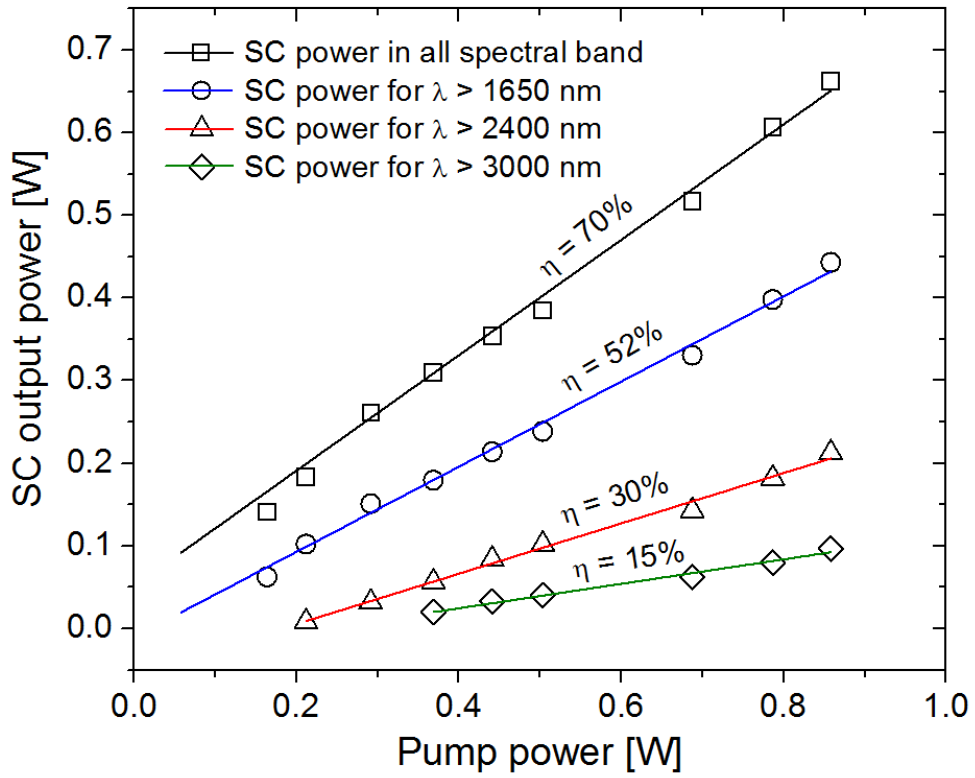

Figure 4-4: Average SC Output Power as a Function of Incident Pump Power (η – Slope Efficiency).

The output power increases linearly with the increase in pump power and was only limited by the available pump power. For 0.86 W of the pump power the SC power as high as 0.66 W in the whole wavelength range with a slope efficiency of 70% was recorded. A distribution of SC power in different spectral bands is presented in Table 4-3. It can be noticed that over 60% of the power corresponded to wavelengths longer than 1.65 µm and 15% (0.1 W) of the power was detected for wavelengths longer than 3 µm.

Table 4-3: SC Power Distribution in Different Spectral Bands.

Spectral Range	Output Power	% of Output Power
All Range	0.66 W	100%
λ > 1.65 µm	0.44 W	66.7%
λ > 2.4 µm	0.21 W	31.8%
λ > 3 µm	0.10 W	15.2%

The measured SC output spectra, recorded for selected pump power levels and corrected for the spectral responsivity of the HgCdTe detector and the monochromator gratings response are presented in Figure 4-5. The inset in each figure depicts the spectrum of light generated at the SMF output. For pump power of 150 mW the output SC spectrum with a characteristic peak at 1.55 µm spreads from ~ 1.4 µm to 1.9 µm (Figure 4-5(a)). In the spectrum of pump signal, presented in the inset, two sets of side lobes spaced symmetrically from the signal at 1550 nm by ~ 25 nm can be distinguished. This spectral signature is characteristic for MI process leading to the break of pump pulses propagating through the SMF into many

shorter sub-pulses and consequently, to the spectrum broadening along with increasing the pump power [34]. Applying the pump power of 300 mW results in the spectrum broadening from ~ 1.4 µm to 1.9 µm and from ~ 1 µm to 3 µm, measured after SMF and ZBLAN fiber, respectively (Figure 4-5(b)). The output SC power for this case was 260 mW. Further increase in pump power leads to further broadening of the output spectrum. For the maximum applied pump power of 860 mW, the 3-octave spanning (from ~ 0.9 µm to 3.6 µm) SC output spectrum generated out of the ZBLAN fiber was obtained (Figure 4-5(d)). It is worth noting here that the pump signal propagating in the SMF was broadened to ~ (1.4 – 2.2) µm. A 10 dB level flatness was obtained in the wavelength interval from ~ 1 µm to 2.7 µm (1700 nm of spectral span). Assuming 20 dB changes in intensity distribution, the spectrum spreads from ~ 1 µm to 3.45 µm (span of 2450 nm). One can see that the intensity falls rapidly for wavelengths longer than 3.4 µm, which can be attributed to the increase in the fluoride fiber attenuation (Figure 4-2).

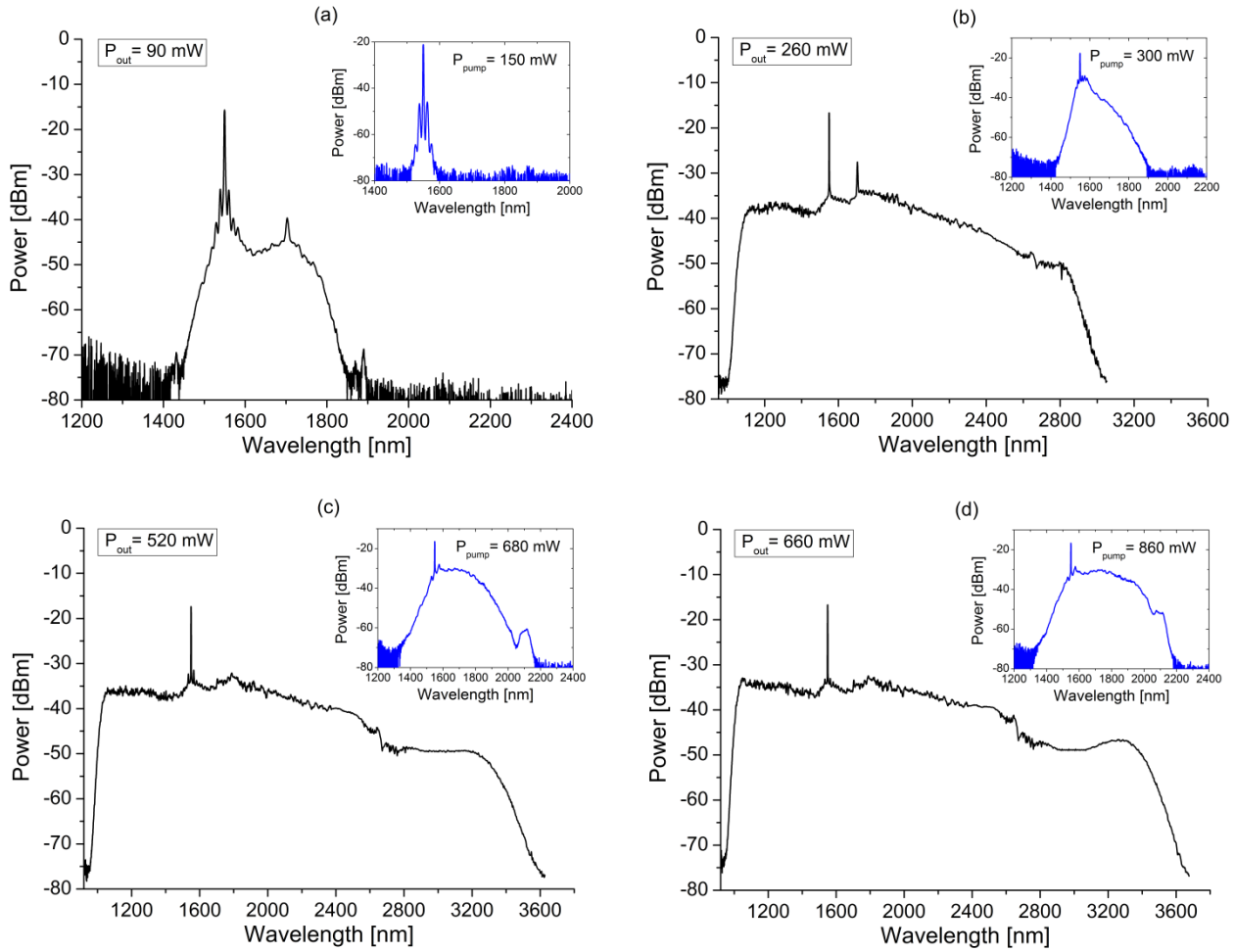

Figure 4-5: Evolution of Output SC Spectrum with Pump Power. Power launched into the ZBLAN fiber: 150 mW (a), 300 mW (b), 680 mW (c), 860 mW (d). Insets present spectrum generated at the SMF output.

As it was mentioned earlier, the initial spectrum broadening in the SMF is caused by MI effect and Soliton Self-Frequency Shift (SSFS) [16],[40],[41]. In the fluoride fiber, the SSFS phenomenon is also responsible for further broadening the spectrum towards longer wavelength while SPM is responsible for blue-shifting of the spectrum [40].

4.2.1.1.4 SC Generation with the Use of Tm-Doped Fiber Amplifier

The general concept of the second experiment was to extend the output SC spectrum only towards mid-IR ($\lambda > 2$ µm). Like in, for example [42]-[44], the active fibers played a role of both non-linear and amplification media. The power of signal initially broadened into the SMF (as high as 0.89 W, of which 58 mW corresponded to $\lambda > 2.4$ µm) was launched to the core of the first TDFA. It allowed absorbing of almost entire pump radiation at 1550 nm and its Raman-scattering components of the wavelength < 1.8 µm by Tm^{3+} ions and finally converting it into longer wavelengths lying in amplification bands of TDF (the first one extends from ~ 1.8 µm to 2.1 µm and the second one from ~ 2.2 µm to 2.5 µm). Applying a Tm-doped fibers as non-linear media allowed us to extend the spectrum from ~ 1.8 µm to ~ 2.7 µm at 40 dB below the peak with 2.37 W for $\lambda > 1.65$ µm and 0.49 W for wavelength beyond 2.4 µm. This spectral extension can be attributed to parallel amplification in both emission bands of Tm^{3+} ions in a silica host. Detailed description of the results can be found in [2]. The radiation generated out of the second TDFA was coupled to the ZBLAN fiber, the same as described in Section 4.2.1.1.1, by bulk optics allowing for launch efficiency of 60%.

The output SC power versus the launched pump power is shown in Figure 4-6. The output power increases linearly along with the pump power increase. The total SC average power of 288 mW is achieved for the launched power of 790 mW. By using different long-pass filters cutting below 1.65, 2, 2.4, 3 and 3.6 µm, it was possible to determine the SC power distribution in different spectral bands, as is presented in Table 4-4. The power as high as 266 mW constituting 92% of total SC output power corresponds to mid-IR spectral band ($\lambda > 2$ µm). The pump-to-signal conversion efficiency was 22.9% with respect to the launched pump power. The power of over 160 mW (58% of total SC output power) lies in wavelengths beyond 3 µm leading to an efficiency of 18.6%.

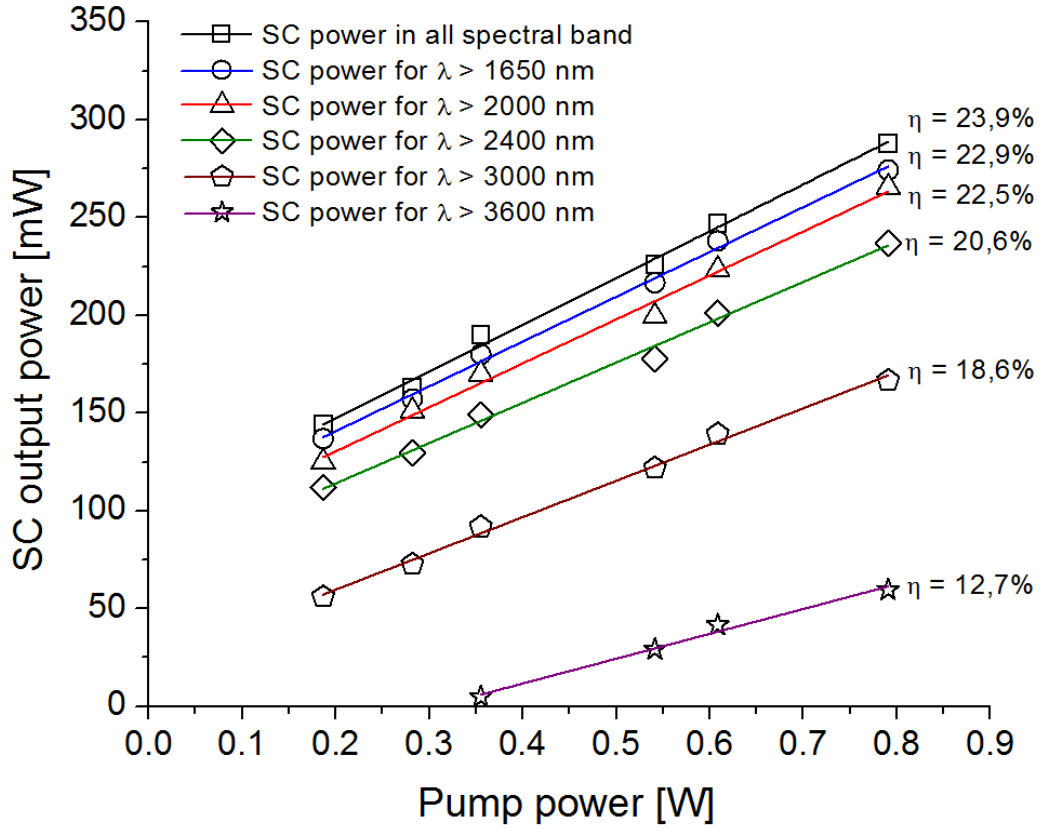

Figure 4-6: Average SC Output Power vs. Launched Pump Power (η – Slope Efficiency).

Table 4-4: SC Power Distribution in Different Spectral Bands.

Spectral Range	Output Power	% of Output Power
All range	288 mW	100%
$\lambda > 1.65$ µm	274 mW	95%
$\lambda > 2.0$ µm	266 mW	92%
$\lambda > 2.4$ µm	240 mW	83%
$\lambda > 3.0$ µm	167 mW	58%
$\lambda > 3.6$ µm	60 mW	21%

The evolution of SC spectrum generated in the fluoride fiber is depicted in Figure 4-7. The inset shows the spectrum generated by the second TDFA at its maximum performance. Higher power generated by the cascade of TDFAs corresponds to higher average SC output power and larger SC spectrum extension limited by fluoride glass transparency. As can be seen, the spectrum spreads from ~ 0.9 µm to 4 µm, however, it is mostly broadened towards infrared wavelengths. The spectrum covers the range of ~ (1.9 – 3.8) µm constituting an octave-spanning mid-IR SC when measured within -25 dB level with respect to the maximum peak. The dip in the spectrum around 2.7 – 2.9 µm corresponds to OH ions absorption in the medium. Another characteristic feature of the spectrum is that it reveals a maximum peak at ~ 3.7 µm, which shows that the light was efficiently converted towards mid-IR (58% of total output power was recorded for $\lambda > 3.0$ µm) and further spectral broadening was difficult due to the rapidly increasing fiber attenuation > 100 dB/km at ~ 4 µm and > 1000 dB at 4.5 µm (Figure 4-2), caused longer wavelengths generated in a 20-m long fluoride fiber to be highly attenuated preventing red wavelengths cut-off extension. Besides, a fiber bend-induced loss contributed to the overall attenuation due to the fluoride fiber was coiled on a 20 cm diameter spool.

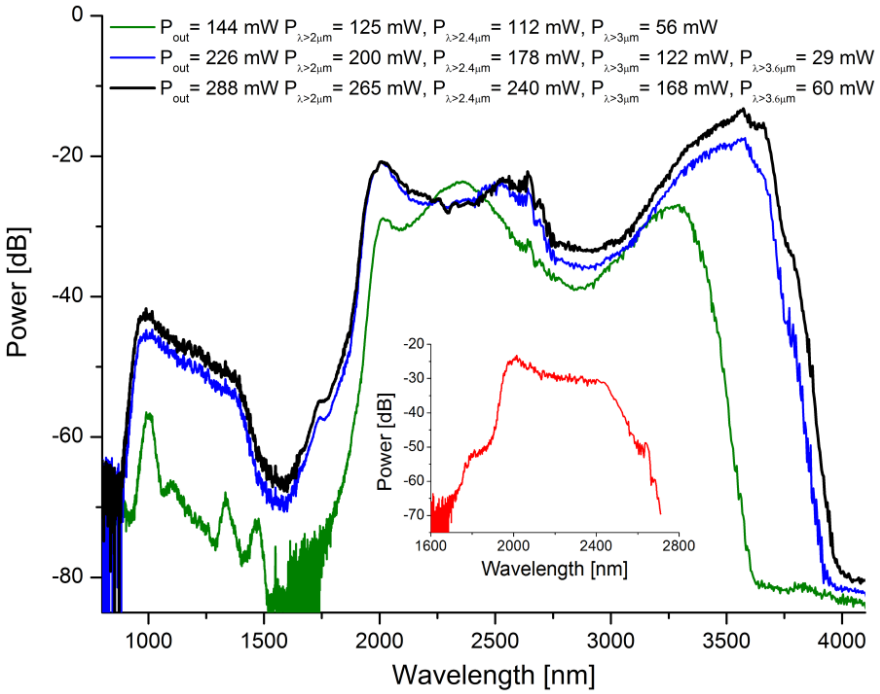

Figure 4-7: SC Spectrum After Propagation Through ZBLAN Fiber, for Selected Values of Output Power. Inset: Spectrum generated by cascade of TDFAs (pump signal) at its maximum performance.

The ZBLAN fiber used has its ZDW at ~ 1.9 µm so that it was mostly pumped in anomalous Group Velocity Dispersion (GVD) region, which means that the main non-linear process leading to spectrum extension is MI effect responsible for solitons formation and soliton self-frequency shift [16],[40]. As the MI process is noise driven, a distribution of many solitons, with different energies are created, resulting in different rates of self-frequency shifting. They are additionally broadened by Self-Phase Modulation (SPM) and Cross-Phase Modulation (XPM) making the SC spectrum relatively smooth and flat. However, as can be seen in Figure 4-7, the spectrum also broadens towards shorter wavelengths (in the band of ~ 0.9 to 1.6 µm) with the average power of 14 mW (only 5% of total output power). It is associated with generation of phase-matched dispersive waves at wavelengths shorter than the ZDW accompanying the MI-induced solitons propagating in the fiber [45]-[47].

In conclusion, we report broadband low-power SC generation in a single-mode fluoride (ZBLAN) fiber with a core/clad diameter of 7/125 µm. When the fiber was pumped by 0.86 W of average power delivered by the 1.55 µm MOPA system, the produced continuum covered 3 octaves from ~ 0.9 µm to 3.6 µm with 0.66 W of average output power. Expending the pump system by applying a cascade of TDFAs providing the average output power as high as 2.37 W in a spectral band of ~ (1.75 – 2.7) µm it was possible to extend the spectrum generated in the ZBLAN fiber from ~ 0.9 µm to 4 µm. The average power as high as 288 mW was recorded, of which 266 mW corresponded to wavelengths longer than 2 µm. Contrary to the first experiment, the output spectrum was mainly distributed towards mid-infrared, the -25 dB bandwidth (measured from the top peak) covers the span of 1900 nm, from ~ 1.9 µm to 3.8 µm.

The difference in the spectrum evolution between the two experiments carried out can be attributed to different spectral bands of the pump signal. In case of the first system, significant part of the pump was located in the normal GVD region of the ZBLAN fiber thus supporting the spectrum extension towards shorter wavelengths with much contribution from SPM. Contrary to that, the second system was mostly pumped in anomalous GVD region and the output spectrum extended mainly towards mid-IR, as a result of Raman induced scattering.

4.2.1.2 Mid-IR Supercontinuum Generation in a ZBLAN Fiber Pumped by a Gain-Switched Tm-Doped Fiber Laser and Amplifier System

Contributors to this section: Jacek Swiderski[2], Maria Michalska[2], Gwenael Mazé[3], Christelle Kieleck[4], Marc Eichhorn[4]

In this section, covered partly in *Optics Express* 21, pp. 7851-7857 (2013), we demonstrate a novel method of Mid-Infrared (MIR) Supercontinuum (SC) generation with the use of a 2 µm gain-switched thulium-doped fiber laser. SC radiation ranging from ~ 1.8 µm to 4.15 µm, generated in a single-mode ZBLAN fiber with a zero-dispersion wavelength (ZDW) shifted to ~ 1.9 µm, is reported. An average output power of 1.25 W with 0.6 W at wavelengths longer than 2.4 µm was measured. It is, to the best of our knowledge, the first report on such an approach to generate a MIR SC in fluoride fibers.

4.2.1.2.1 SC Experimental Set-Up

The SC source consists of a 1.55 µm fiber MOPA, a gain-switched Thulium-Doped Fiber Laser (TDFL) and a Thulium-Doped Fiber Amplifier (TDFA). The principal scheme of this configuration is shown in Figure 4-8.

[2] Institute of Optoelectronics, Military University of Technology, 2 Kaliskiego Street, 00-908 Warsaw, Poland.

[3] Le Verre Fluoré, Campus KerLann, F-35170 Bruz, Brittany, France.

[4] French-German Research Institute of Saint-Louis ISL, 5, rue du Général Cassagnou, B.P. 70034, 68301 Saint-Louis Cedex, France.

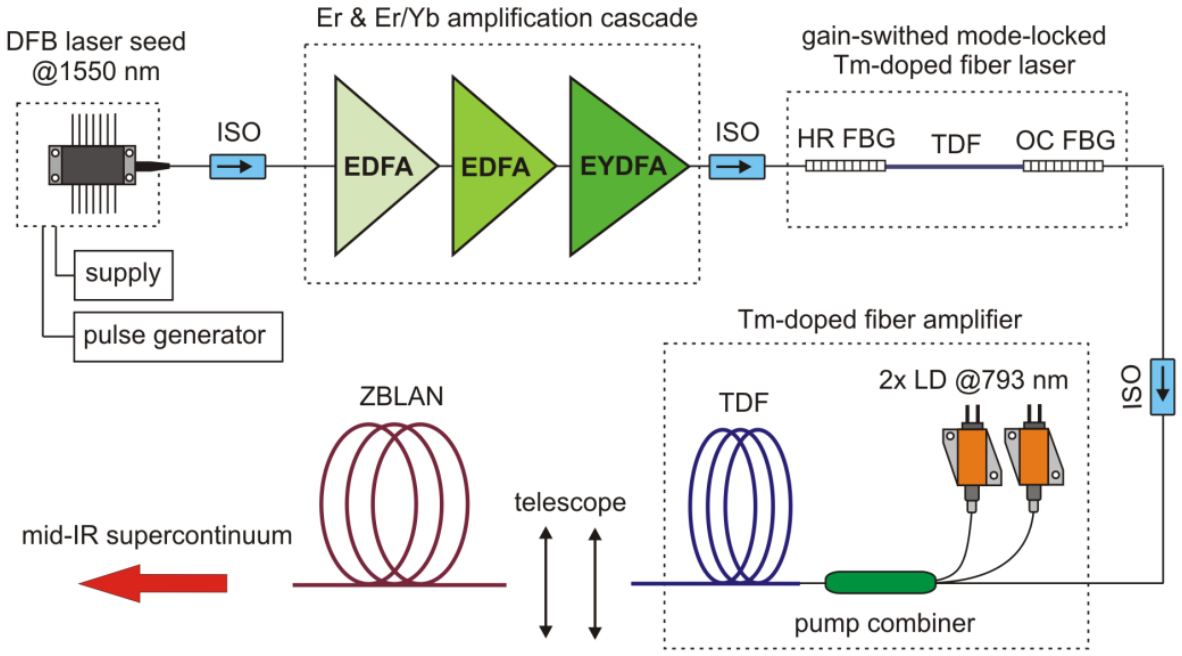

Figure 4-8: Block Diagram of Fiber Mid-IR SC Source. ISO – Optical Isolator.

To obtain a stable pulse train, fast gain-switching and resonant pumping are required. In-band pumping ensures a rapid population inversion that can be depleted by a single short gain-switched pulse. Then the cross-relaxation and excited state absorption processes can be reduced leading to generation of stable, short 2-µm pulses, as was shown in [48]. Furthermore, in gain-switched TDFLs, an output pulse duration is determined by an active medium gain and the round-trip time, which means that the length of active fiber directly affects output time characteristics of a laser. In such a situation, only core-pumping can provide a suitable gain while keeping a resonator length short and thus supports generation of short (tens of ns) pulses [48]. For this reason, a ~ 20-cm long, single-mode double-clad, Tm-doped (~ 2 wt. %), silica fiber (TDF) was used as an active medium of the GSML laser. It had a 10/130 µm core/clad diameter and a corresponding numerical aperture NA of 0.15/0.46. The active fiber was core-pumped by a 1.55 µm fiber MOPA system, delivering pulses of 20 – 700 ns duration at the frequency independently changeable in the range from 26 to 320 kHz.

The MOPA system consisting of a DFB laser seed followed by a cascade of Erbium- and Erbium:Ytterbium-Doped Fiber Amplifiers (EDFA and EYDFA) was capable to deliver pulses with energy of several tens of µJ and average power of up to 3.5 W. About 90% of pump power was absorbed by the active dopant. The output from the MOPA system was directly spliced to the pigtail of a 3-cm long High Reflector (HR) Fiber Bragg Grating (FBG). The laser cavity was formed by a HR FBG having a reflectivity of > 99% at 1994.5 nm, and an Output Coupler (OC) FGB with a reflectivity of 90% at 1994.6 nm and a 3 dB reflection bandwidth of 1.5 nm. The FBGs were cleaved and fusion spliced very close to the active fiber to keep the resonator short. In the next step, the TDFL output was optically isolated and spliced to an input of TDFA that was built with the use of ~ 2.5-m long TDF, characterized by the same parameters as mentioned above. The amplifier was cladding-pumped by two fiber-pigtailed 4.75 W 790-nm pump laser diodes with 105 µm core diameter and 0.22 NA via a (2 x 1) + 1 pump combiner with a signal feedthrough. Finally, the 2 µm amplified pulse train was launched into a ZBLAN fiber with the use of a telescope allowing for coupling efficiency of ~ 60%. The 20-m long ZBLAN fiber (manufactured by Le Verre Fluoré) had a core/clad diameter of 7/125 µm and a NA of 0.23. The ZDW and cut-off wavelength of this fiber were 1.9 µm and 2.04 µm, respectively. Both ends of the fluoride fiber as well as the output fiber end of the TDFA were polished at an angle of 8° to avoid any back reflections.

The benefit of using the GSML Tm^{3+}-doped fiber laser as a pump source is the lower cost and reduced complexity of the system, compared to, for example Q-switched or QML lasers. Besides, comparing with CW pumping scheme, the increased peak power of self-mode-locked pulses, amplified in a chain of fiber amplifiers, can eliminate the critical dependence on the ZDW, as it was reported in [49].

SC spectrum from 1.2 µm to 2.4 µm wavelength was measured by using an Optical Spectrum Analyzer (OSA), whereas the longer wavelengths were measured with a grating monochromator and a thermoelectrically cooled HgCdTe detector. A sampling digital oscilloscope with 6 GHz bandwidth and two detectors with rise/fall time of < 35 ps were used to measure time characteristics.

4.2.1.2.2 Experimental Results and Discussion

The gain-switched TDFL was pumped by ~ 100 ns 1.55 µm pulses with the energy of up to 80 µJ at the Pulse Repetition Frequency (PRF) ranging from 26 to 40 kHz. After reaching the lasing threshold, the 2 µm output pulses of long duration appeared and with the increase in pump power both the pulse build-up time and pulse width shortened. Further increase in pump energy led to Mode-Locked Resembling (MLR) operation with a full modulation depth, which is shown in Figure 4-9.

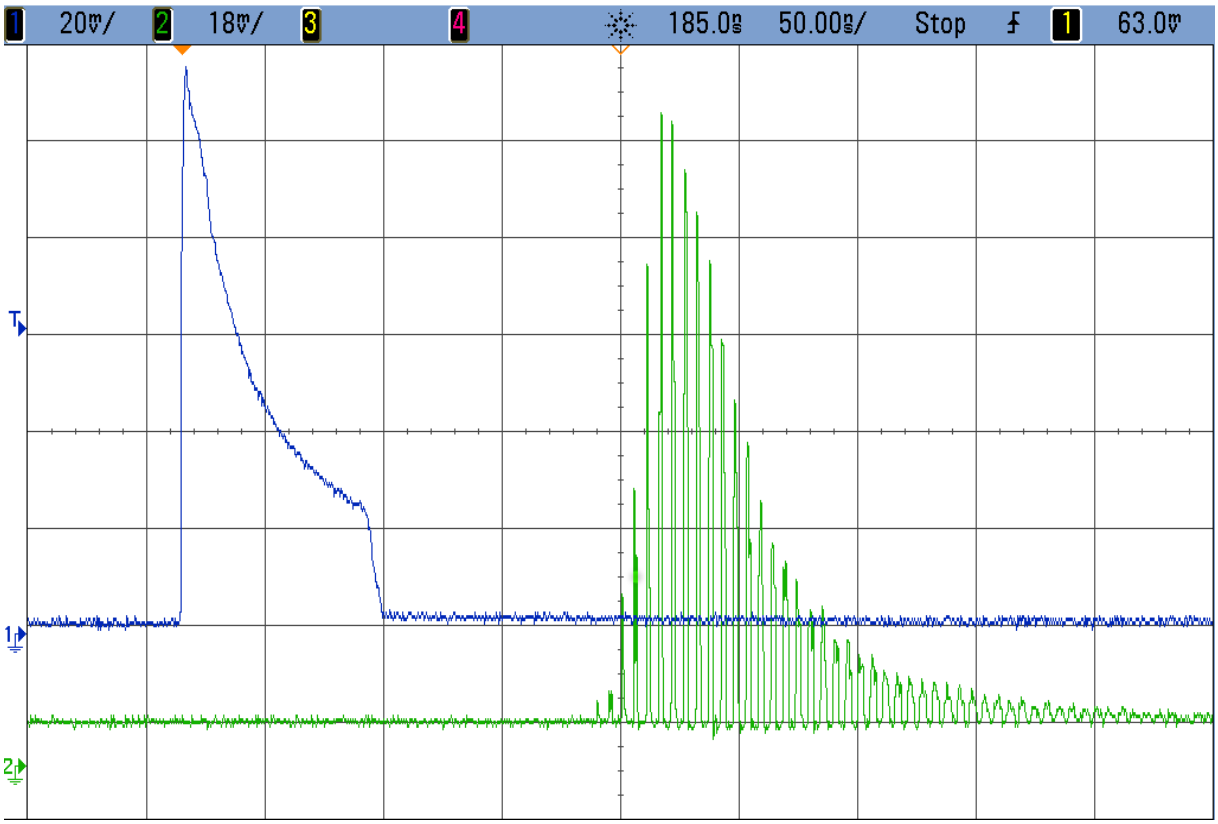

Figure 4-9: An Example of Oscilloscope Picture of Recorded Gain-Switched Mode-Locked-Like Output Laser Pulse. Trace 1 (upper) – pump 1.55 µm pulse; Trace 2 (lower) – output 2 µm laser pulse.

The envelope width of the gain-switched pulse was ~ 50 ns, whereas the duration of the most intensive sub-pulses was 200 – 300 ps (190 MHz spectral space), the time of which is much shorter than the laser cavity round-trip time (5.3 ns). The mode-locking depth as well as the exact form of generated pulse train was strictly dependent on the pumping conditions (PRF, pump pulse width and shape, pump pulse energy).

We believe that the origin of self-starting MLR operation in our gain-switched fiber laser is the beating effect of laser longitudinal modes [50].

In the next step, the MLR pulses from the gain-switched fiber laser (presented in Figure 4-9) were boosted in the TDFA. Figure 4-10 shows the evolution of output average power at 2 µm for the PRF of 26 kHz and 40 kHz as a function of TDFA pump power. For 26 kHz (Figure 4-10(a)), the average power of 2.3 W, with corresponding 88 µJ energy in 50 ns duration gain-switched pulse was measured. Increasing the PRF to 40 kHz results in average power scaling up to 2.6 W with a corresponding pulse energy of 65 µJ (Figure 4-10(b)). The amplifier operated with a 26.5% and 31% slope efficiency for 26 kHz and 40 kHz, respectively.

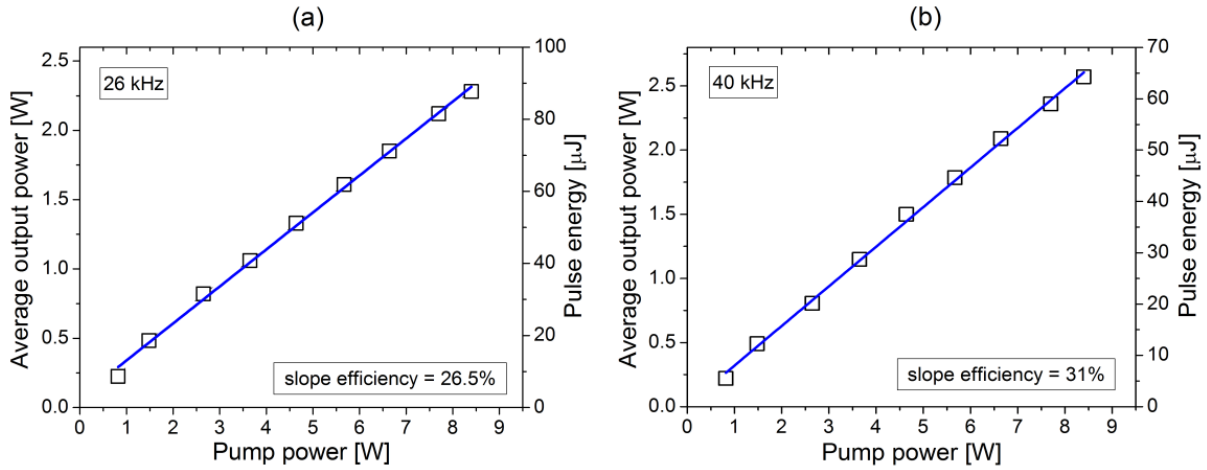

Figure 4-10: Average Output Power at 2 µm Wavelength for 26 kHz (a) and 40 kHz (b) vs. Launched TDFA Pump Power.

Figure 4-10 presents pulse energy and peak power for selected MLR pulses in a 50-ns gain-switched envelope for the PRF of 26 kHz. The inset presents a typical MLR pulses within an envelope of a gain-switched pulse. During the experiment we did not carry out autocorrelation measurements and the pulse structure was recorded with the use of a sampling oscilloscope and a fast photodiode and then analyzed in OriginPro software. The timing of the sub-pulses was slightly unstable, owing to amplitude fluctuations of 1.55 µm pump pulses. Furthermore, we also noticed that careful adjustment of the pump power and the pump pulse time characteristic led to the improvement of output pulse structure stability.

As can be seen in the inset in Figure 4-11, the width of the first and last sub-pulses was longer than those in the center of the gain-switched envelope. The highest peaks were characterized by the shortest duration and thus the highest peak-power. The generated pulse train consisted of ~ 15 – 20 sub-pulses. The maximum energy of the gain-switched pulse (calculated by dividing the average output power by the PRF) was 88 µJ, whereas the energies of three highest MLR peaks (marked in the inset as 4, 5 and 6) were 8.3 µJ, 13.7 µJ and 15.7 µJ (with corresponding peak power of 22.2 kW, 24.7 kW and 27.8 kW), respectively.

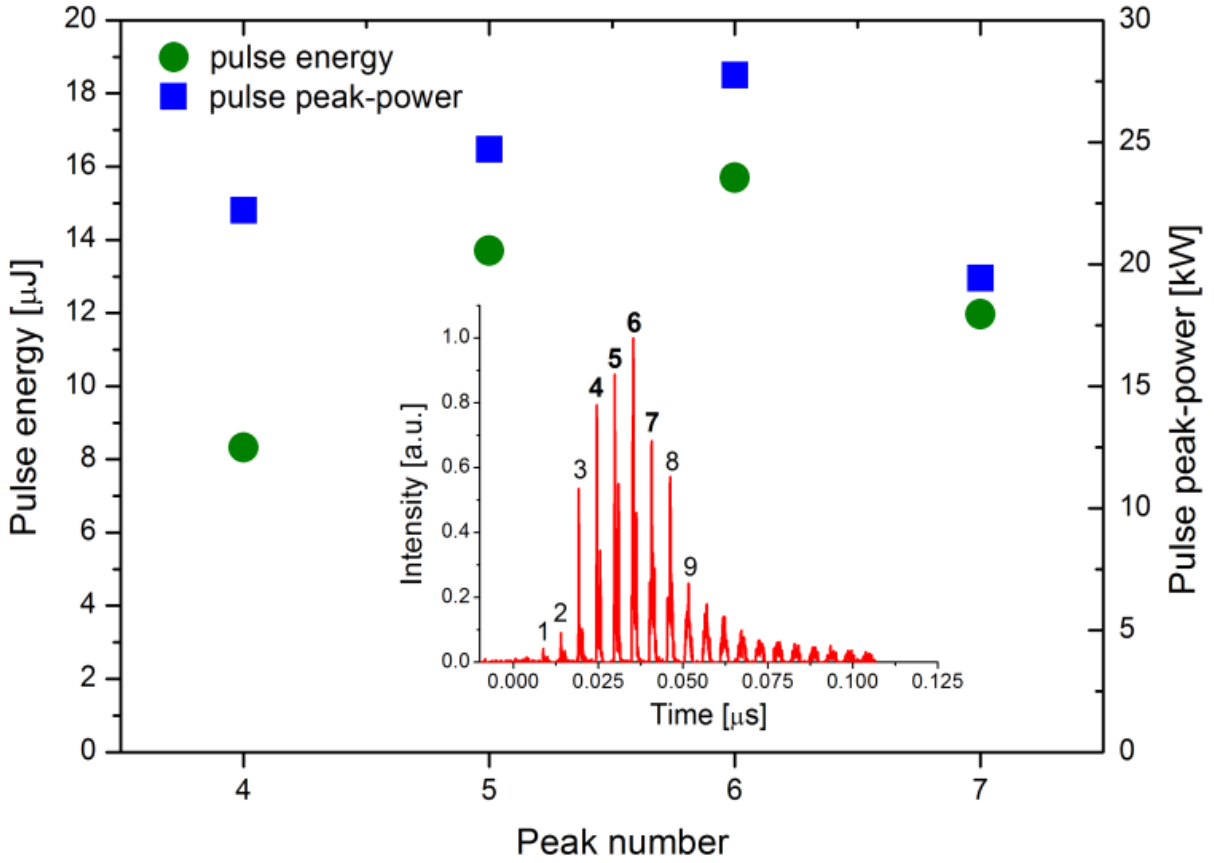

Figure 4-11: Pulse Energy and Peak Power for Selected MLR Sub-Pulses in a Gain-Switched Pulse Envelope (Inset).

Finally, the amplified pulse train was launched into the ZBLAN fiber with ~ 60% coupling efficiency. As was mentioned earlier, the fluoride fiber had the ZDW at 1.9 μm in order to be pumped in anomalous dispersion region but relatively close to the ZDW, which facilitates spectral broadening towards mid-IR [40]. The output SC power as a function of launched pump power, for both PRFs applied, is shown in Figure 4-12. The output power increases linearly with the increase of pump power and was only limited by the available pump power. For instance, for 26 kHz increasing the incident pump power to 1.23 W results in the total SC power of 0.74 W, out of which 0.27 W is in the wavelength range beyond 2.4 μm. Over 0.12 W was detected for $\lambda > 3$ μm. When operating at 40 kHz, the output power was as high as 0.9 W, where 240 mW and 86 mW were measured for $\lambda > 2.4$ μm and 3 μm, respectively. The slope efficiency η of generated SC in all spectral SC band was 62.8% and 60% for the PRF of 40 kHz and 26 kHz, respectively. Even though higher PRFs provided higher generation efficiency of total output power, the generation efficiency of longer wavelength radiation was higher for lower PRF, being a consequence of higher peak power of pump pulses.

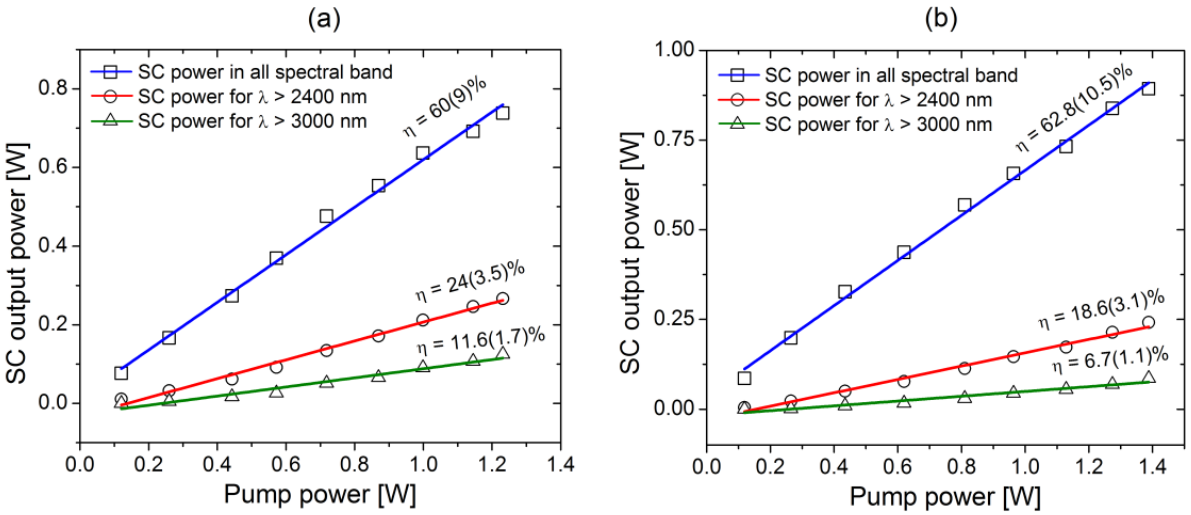

Figure 4-12: Average SC Output Power for 26 kHz (a) and 40 kHz (b) vs. Launched Pump Power. Slope efficiencies η in brackets indicate slope efficiency with respect to TDFA pump power.

The measured SC output spectrum, corrected for the spectral responsivity of the HgCdTe detector and the monochromator gratings response, is presented in Figure 4-13.

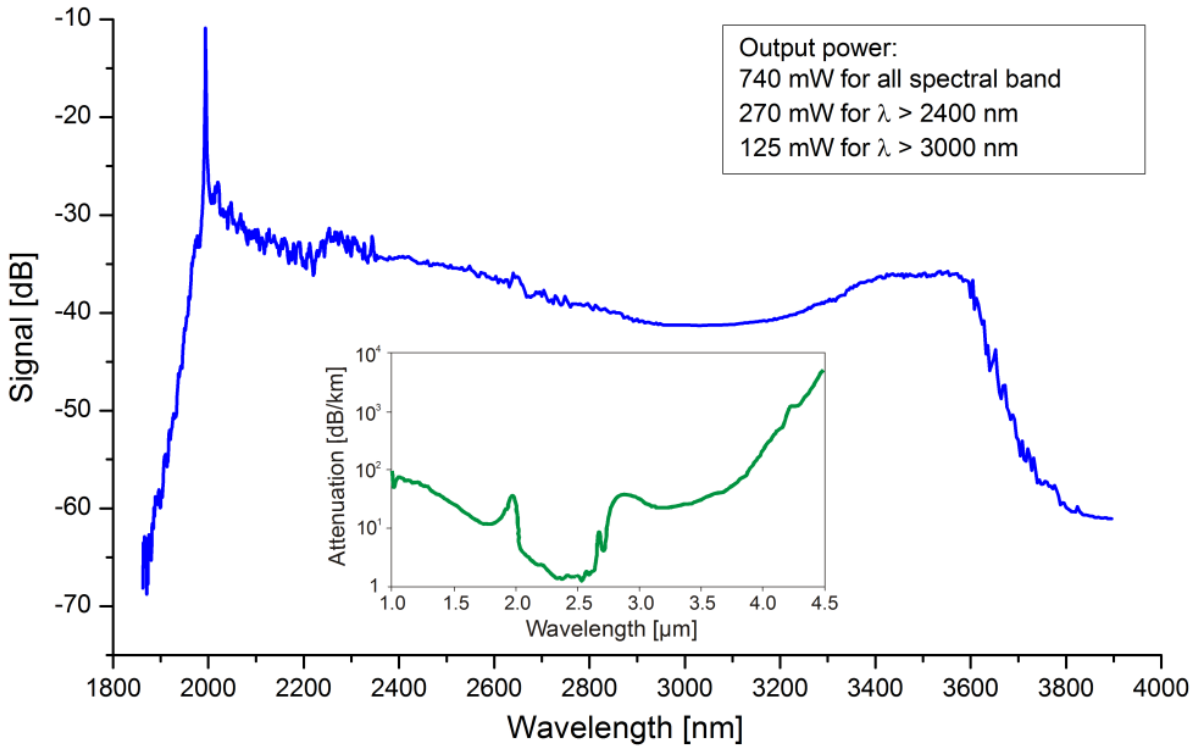

Figure 4-13: SC Spectrum After Propagation Through the ZBLAN Fiber for the Maximum Output Power and the PRF of 26 kHz. Inset: Attenuation of the ZBLAN fiber.

A modulation instability effect leading to the creation of solitons and then soliton self-frequency shift are mostly responsible for spectrum extension in Figure 4-13, which is typical for pumping a non-linear medium

in the anomalous Group Velocity Dispersion (GVD) region [16],[22],[40]. Additionally, the red-shifted solitons were broadened by self-phase modulation and cross-phase modulation, making the SC spectrum smooth and flat. As can be seen in Figure 4-13, the 10 dB flatness of spectral intensity was maintained in the wavelength interval from ~ 2100 to 3600 nm (span of 1500 nm). Another characteristic feature of the spectrum is that it is mainly broadened towards longer wavelength with reference to the pump wavelength, in contrary to spectra obtained in laser systems utilizing 1.55 µm pulses and pumping in the normal GVD of ZBLAN fibers [e.g. [15],[16],[22],[33]]. Further spectral broadening towards mid-IR was difficult due to the rapidly increasing fiber attenuation > 100 dB/km at ~ 4 µm and > 1000 dB at 4.5 µm (inset in Figure 4-13), such that red wavelengths generated in the fluoride fiber were highly attenuated preventing long wavelengths cut-off extension. The length of the ZBLAN fiber used in the experiment was not optimized. It will be the subject of further investigation, taking into account the pump pulse characteristics of our laser source. As was shown for example in [15], by proper selection of fluoride fiber length with regard to pump pulse peak power the inherent material losses of a fiber can be overcome leading to spectrum extension even beyond 6 µm.

In the next experiment we decided to scale up the output SC power. To this end, we modified the TDFA section by using a ~ 4.5-m long Large-Mode-Area (LMA) Tm-Doped Fiber (TDF) characterized by a core/clad diameter of 25/250 µm and corresponding numerical apertures of 0.1/0.46. It was cladding pumped in co-propagation configuration by a 793-nm, 30-W laser diode, which radiation was launched into the gain fiber via a (2 + 1) x 1 pump combiner with a signal feedthrough (signal input port: 10/125 µm, 0.15/0.46 NA; pump input ports: 105/125 µm, 0.22 NA; output port: passive double-clad 25/250 µm fiber, 0.11/0.46 NA). The output of the LMA TDF was first equipped with a home-made mode field adaptor (fiber taper) with a 25/250 µm (0.11/0.46 NA) fiber at the input and 11/125 µm (0.11 NA) fiber at the output, providing the mode conversion to a single mode fiber (0.5-m long SM2000). The maximum average output power provided by the 2 µm laser system, measured at the SM2000 fiber output, was 4.8 W. All the pump system components were fusion spliced, thus making it all-fiber. Finally, the 2 µm amplified pulses were launched into the ZBLAN fiber. The output spectrum generated from the ZBLAN fiber, for maximum recorded output SC power, is presented in Figure 4-14. The inset presents SC average output power recorded in different bands vs. launched pump power.

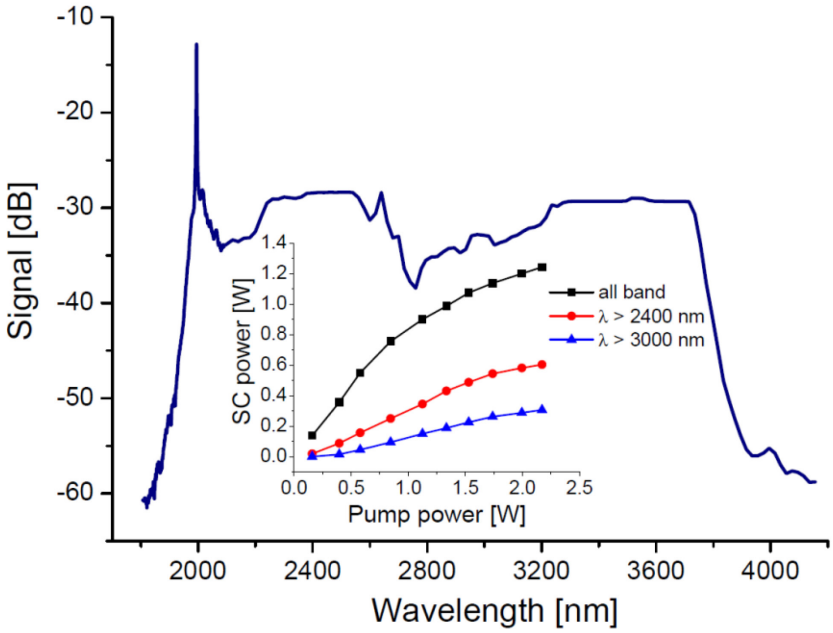

Figure 4-14: SC Emission Spectrum Generated in the ZBLAN Fiber. The inset shows SC power evolution in different spectral bands as a function of lunched pump power.

As can be seen in Figure 4-14, the spectrum covers more than one octave in frequency that is from ~ 1.8 µm to 4.15 µm with a residual peak at the pump wavelength. The maximum average output power was measured to be 1.25 W, for ~ 2.2 W of launched pump power. It can be noticed that 48.5% of the power (0.6 W) corresponded to wavelengths longer than 2.4 µm and 24.6% (0.31 W) of the power was detected for wavelengths longer than 3 µm. The dip in the spectrum around 2.8 µm corresponds to OH ions absorption in the non-linear medium and detection system. The 10 dB spectral flatness was maintained in the range of ~ 2 µm to 3.8 µm. The pump light peak at 1994.5 nm was not included into the calculation of the bandwidth.

In conclusion, we have demonstrated for the first time, to the best of our knowledge, an over octave spanning MIR supercontinuum generation in a step-index ZBLAN fiber, pumped by a gain-switched Tm^{3+}-doped fiber laser and amplifier system. The pump laser delivered ~ 50 ns gain-switched pulses with simultaneously mode-locked resembling sub-pulses. The maximum SC output average power for 26 kHz of repetition rate was 1.25 W and the power beyond 2.4 µm and 3 µm were measured to be 0.6 W and 0.31 W, respectively. Both an output power and spectrum width can be further scaled up.

4.2.1.3 Actively Q-Switched and Mode-Locked Tm^{3+}-Doped Silicate 2 µm Fiber Laser for Supercontinuum Generation in Fluoride Fiber

Contributors to this section: Michael Eckerle[5], Christelle Kieleck[5], Jacek Świderski[6], Stuart D. Jackson[7], Gwenael Mazé[8], Marc Eichhorn[5]

From: OPTICS LETTERS, **37**, pp. 512-514 (2012)

In this section we demonstrate a diode-pumped actively Q-switched and actively mode-locked Tm^{3+}-doped double-clad silicate fiber laser is reported providing up to 5 W of average output power at ~ 60 kHz Q-switch envelope repetition rate and ~ 8 µJ sub-pulses with up to 2.4 kW peak power. Using this source as a pump laser for supercontinuum generation in a ZBLAN fiber, over 1080 mW of supercontinuum from 1.9 µm to beyond 3.6 µm was obtained at an overall efficiency of 3.3% with respect to the diode pump power.

Supercontinuum fiber lasers based on fluoride glass emitting at eye-safe wavelengths between 2 µm and 5 µm are promising laser sources for countermeasures, spectroscopy, and remote sensing. For mid-infrared SC generation short pulse durations and thus high peak powers are necessary. These pulses break up by modulation instabilities into femtosecond pulses, which create the supercontinuum, e.g. in fluoride glasses [22],[23],[32],[33],[51]. The required pump pulses, usually on the (sub-)nanosecond scale with kW peak powers, are not achievable from fiber lasers by simple Q-switching. Passive mode-locking results in pulse energies that are too low, thus creating a limit in the average power. Up to now, pulsed laser diodes and amplifier schemes were the necessary pump sources for SC generation [22],[32],[33]. To optimize the relation among pulse width, pulse peak power, and accessible pulse energy while providing a simple, one-oscillator solution, active cw Mode-Locking (cw-ML) is a good choice [52]. In addition, active mode-lockers show much higher damage thresholds so that > 10 W of average output power can be achieved [52]. Further scaling of the pulse energy and peak power of the nanosecond to sub-nanosecond SC pump pulses can be achieved by simultaneous intracavity Q-switching of an actively Mode-Locked (Q-ML) fiber laser.

This section presents a simultaneous actively Q-switched and actively mode-locked 2 µm Tm^3 fiber laser in a single-fiber-oscillator arrangement and its use as a pump source for SC generation by pumping a ZBLAN fluoride fiber. Figure 4-15 shows the set-up of the Tm^3 fiber laser. The active medium is a 2.4-m long silica double-clad fiber (from the former Optical Fiber Technology Center, Australia) with a 20 µm diameter

[5] ISL, French-German Research Institute of Saint-Louis, 5 rue du Général Cassagnou, 68300 Saint-Louis Cedex, France.

[6] Institute of Optoelectronics, Military University of Technology, 2 Kaliskiego Street, 00-908 Warsaw, Poland.

[7] Institute of Photonics and Optical Science, School of Physics, University of Sydney, NSW 2006, Australia.

[8] Le Verre Fluoré, Campus KerLann, F-35170 Bruz, Brittany, France.

(NA 0.20) core doped with 2.8% Tm^3. The hexagonally shaped cladding has a flat-to-flat diameter of 300 µm (NA 0.40). The fiber end facing the cavity end mirror is cleaved at an angle of 8° to reduce Fresnel back reflections. The opposite end is cleaved perpendicular to the fiber axis to act as an Output Coupler (OC) with a reflectivity of ~ 4%. The dielectric end mirror of the 0.4-m long free-space external cavity has a high reflectivity about 2 µm. A 50 µm thick etalon with a reflectivity of 90% on both sides was inserted into the cavity to obtain a well-defined output spectrum. An Anti-Reflection (AR)-coated Acousto-Optic Modulator (AOM) mode-locker was placed directly in front of the cavity end mirror. A second AR-coated AOM with a deflection efficiency of > 80% for Q-switching was inserted between the fiber end and the etalon. The high deflection efficiency and the 8° cleave of the fiber ensure a high Amplified Spontaneous Emission (ASE) threshold to obtain a high initial gain before Q switching. The mode-locker was tunable in its drive frequency to allow accurate adjustment to the cavity round-trip time to establish mode-locking.

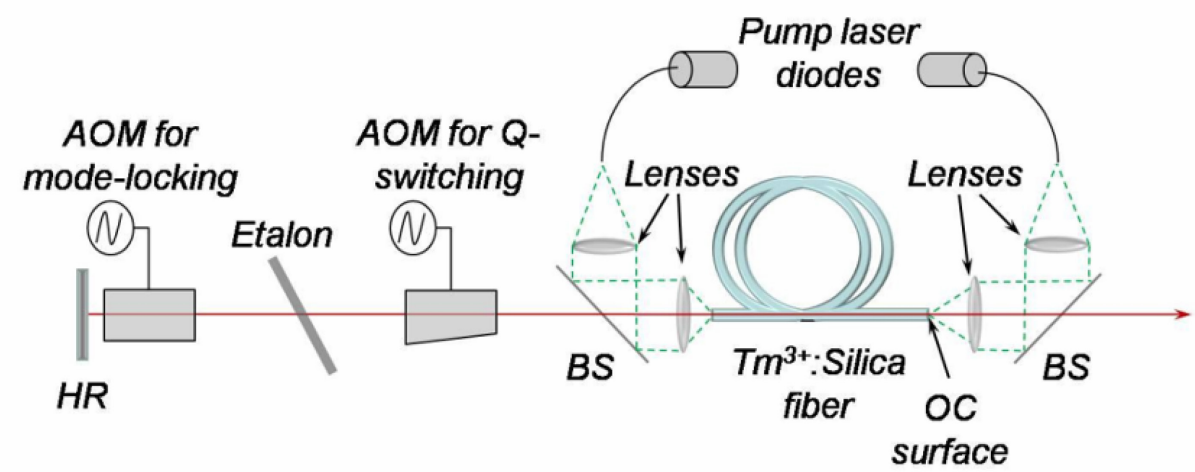

Figure 4-15: Set-Up of the Q-Switched, Mode-Locked Tm^{3+}:silica Fiber Laser.

The fiber was symmetrically pumped at 792 nm using fiber-coupled laser diodes, which each emitted 25 W from a 200 µm multi-mode fiber (NA 0.22). The pump light was collimated using lenses with an effective focal length of 11 mm. Identical lenses were used to focus the pump light onto the fiber and to collimate the fiber laser output at both ends. The lenses were AR coated for the pump and laser radiation. Dichroic mirrors reflective for the pump and highly transmissive for the laser wavelength were used to combine laser and pump light and to direct the pump light onto the fiber. Because of the small core and low NA of the pump fibers relative to the cladding and NA of the laser fiber, a pump launch efficiency of ~ 96% was achieved.

As fiber lasers are extremely sensitive to back reflections, optical isolation was provided by a home-built polarization-independent optical isolator attributable to the non-polarization maintaining properties of the fiber laser. The isolator set-up consisted of splitting the beam into two arms, one for each polarization, which were separately isolated and then recombined. Using half-wave plates placed within the arms, it was possible to change the output power of the set-up while keeping the actual pulse parameters unchanged.

When both AOMs were activated, the laser produced pulse trains with a repetition rate of ~ 60 kHz at an average output power of 5 W. For the Q-ML set-up, mode-locking could be achieved at different ML frequencies and resulted in the pulse widths and average output powers shown in Figure 4-16. There the pulse width [Full Width At Half Maximum (FWHM)] of the strongest sub-pulse in the generated pulse trains and the relative power drop, occurring when switching from simple Q-switched to Q-ML operation, is depicted. This effect, which arises from coupling of non-evenly spaced modes, has already been investigated under cw-ML operation [52]. However, in contrast to the cw-ML results, where for one ML frequency the pulses obtained were < 100 ps, while all other operation points resulted in > 2 ns pulses,

the Q-ML operation provides pulses of 2 ns duration even for the ML frequency in which the drop in average output power is minimal.

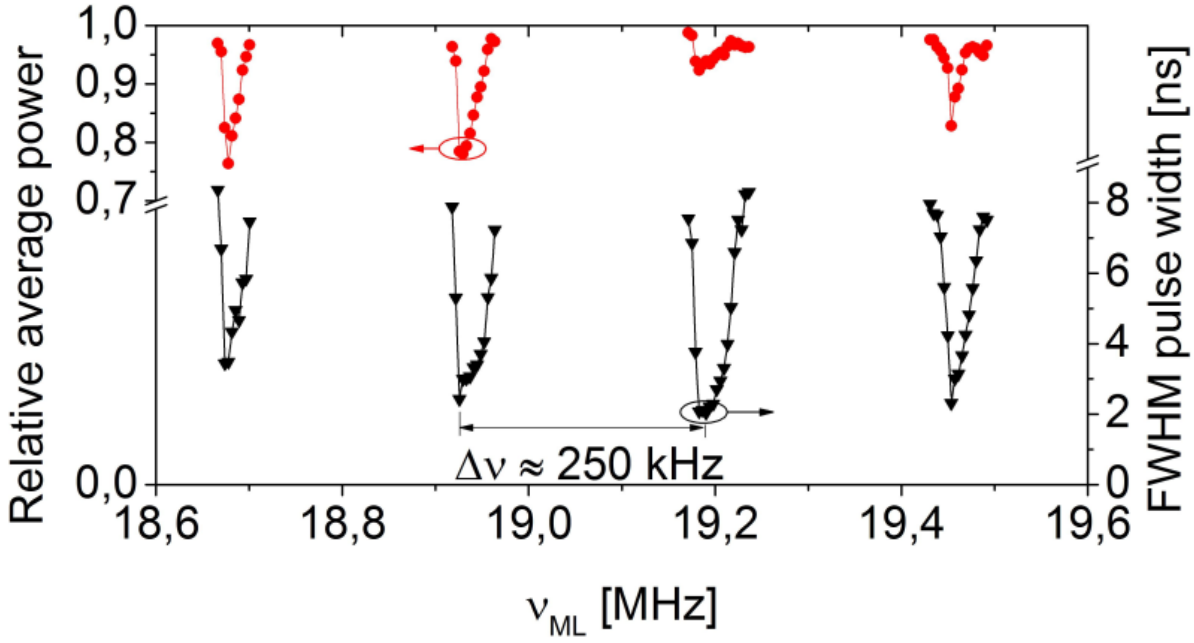

Figure 4-16: Relative Average Power and FWHM Pulse Width of the Major Sub-Pulse in the Q-Switch Envelope for Different Mode-Locking Frequencies.

The pulse trains consisted of 5 – 12 pulses within one Q-switch envelope. The corresponding energies and peak powers of these sub-pulses for ν_{ML} =19.1905 MHz are shown in Figure 4-17. The peak power P_{peak} was calculated under the assumption of a Gaussian pulse shape resulting in $P_{peak} = 0.94\ Ep/\Delta t_{FWHM}$, with Ep being the pulse energy and Δt_{FWHM} the pulse width measured at FWHM. Because of the approximately equal pulse widths within one Q-switch envelope, the distribution function of energy and peak power follows the Q-switch envelope. For the measurement shown in Figure 4-17, the maximum pulse energy was ~ 8 µJ at a peak power of 2.5 kW. After a new alignment and recleaving of the fiber, the maximum pulse energy could be increased to ~ 9 µJ; however, at a larger pulse width thus resulting in a lower peak power of 1.5 kW. The emission peaks of the laser with a spectral width of 1 – 2 nm were located at 1950.7 nm, 1976.6 nm, 2003.5 nm, and 2030.8 nm. The Q-switch envelope phase is not stable with respect to the ML pulse train and the number of sub-pulses can change by ± 1, resulting in pulse-to-pulse fluctuations in peak power ~ 10%.

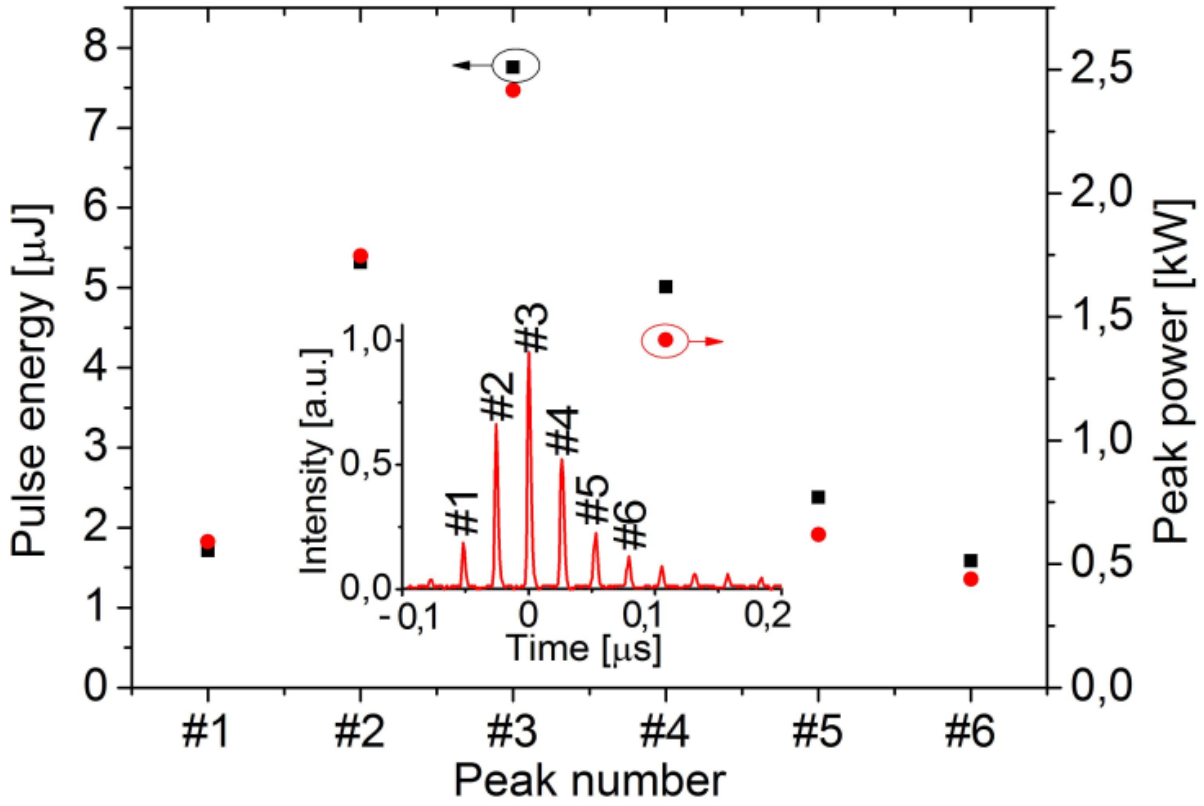

Figure 4-17: Pulse Energy and Peak Power for Succeeding Pulses in One Q-Switch Envelope (Inset).

In a second experiment the Tm^3 fiber laser was used as the pump source for SC generation in a 15-m long ZBLAN fiber with an 8 µm diameter core, a cut-off wavelength of 3.13 µm, and a 125 µm diameter cladding. A fiber with a zero-dispersion wavelength at about 1.54 µm was chosen so that it could be pumped in its anomalous dispersion regime necessary for SC generation. This allows for SC wavelength conversion by four-wave mixing, self-phase modulation, and Raman scattering [32],[51]. The pump was mode matched to the ZBLAN fiber by a telescope, allowing for launch efficiencies of over 60% despite the not optimum beam quality of the pump, caused by the slightly multi-mode nature of the Tm^3 fiber and the recombining after isolation. Using a scanning grating spectrometer, an InAs detector, and a lock-in amplifier for noise reduction and correcting for the overall detection response results in the spectra depicted in Figure 4-18, recorded with a resolution of 6.27 nm. As the InAs detector was the only type available at the time of the experiment, the measured spectra were limited to ~ 3600 nm – see inset in Figure 4-18. Using the optical isolator set-up, the fiber was independently pumped with both polarizations. As can be seen in the inset, there is no clear impact to the conversion efficiency for pumping with different polarizations, in agreement with the fact that the ZBLAN fiber is not polarization maintaining and not exposed to any symmetry breaking constraints. In some cases, however, a p-polarized pump performs better, which can be attributed to slightly different pulses in the two polarizations, e.g. envelope shape and number of sub-pulses, resulting from a symmetry breaking by the angle cleave and the tilted etalon in the free-space cavity of the Q-ML fiber laser.

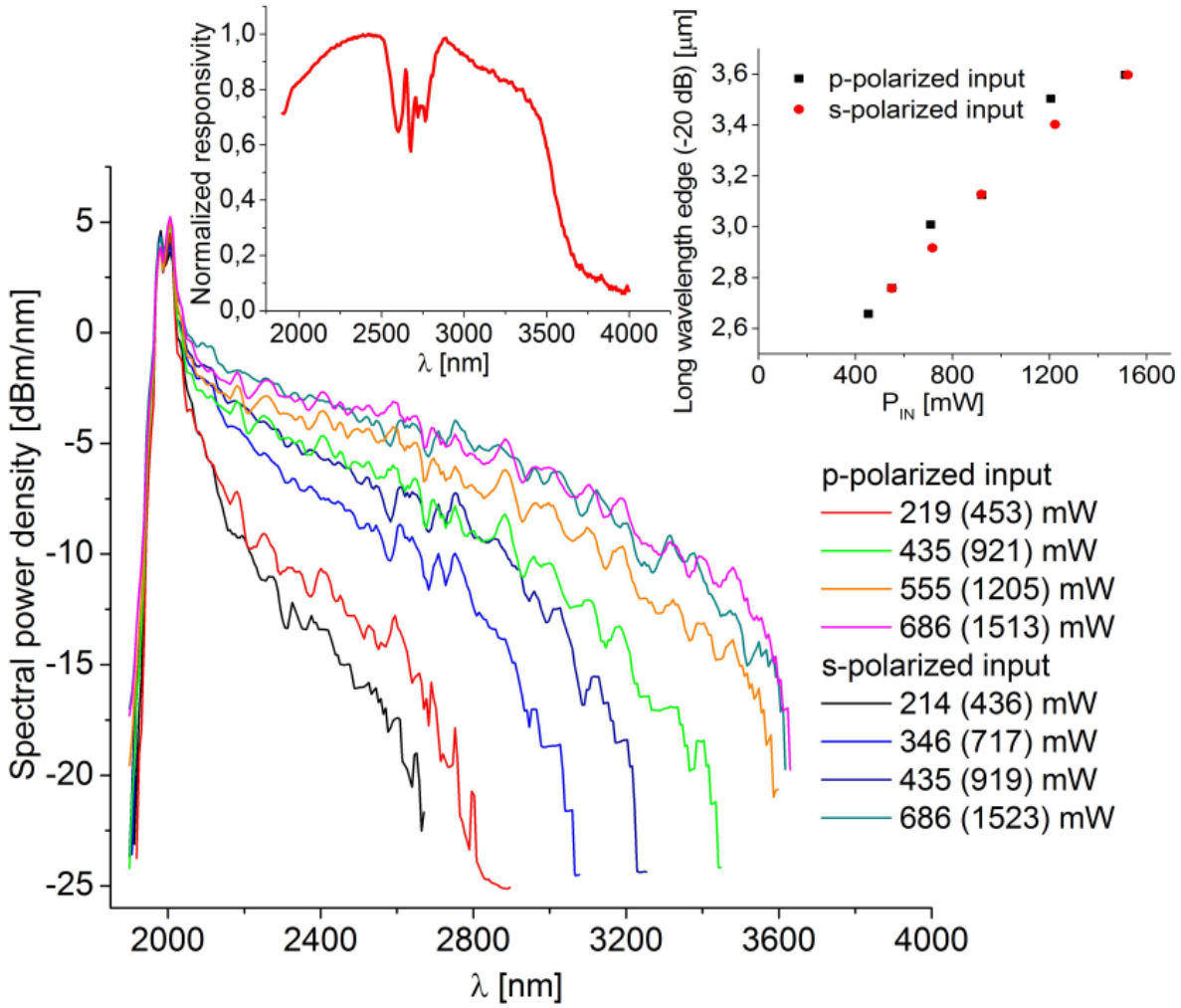

Figure 4-18: SC Output Spectra Resulting from Different Incident Powers from the Q-ML Pump. The value in the legend denotes the overall average output power P_{OUT}, and the value in brackets the corresponding average incident pump power P_{IN}. The right inset shows the wavelength at which the power dropped by 20 db relative to the peak of the spectrum, and the left inset depicts the overall spectrometer response.

Using a long-wave pass filter with a 3 dB edge at 2340 nm, the amount of power shifted beyond 2340 nm was investigated and is depicted in Figure 4-19. Up to ~ 105 mW was measured for $\lambda > 2340$ nm. For comparison the upper inset shows the overall SC power including residual pump, reaching over 700 mW. The black line is a linear interpolation of the first five measurement points. The rollover of the total SC power for input powers larger than 800 mW results from increasing absorption of the fiber for longer wavelengths (see lower inset in Figure 4-19) owing to the 15-m long fiber used. As the fiber was coiled on a 20 cm diameter spool, bend-induced losses contribute, which have been shown to be significant at these long wavelengths even for a radius of 40 cm [33]. Increasing the incident pump power to 3 W resulted in an SC power of over 1080 mW and more than 216 mW beyond 2340 nm. The overall wavelength conversion efficiency from the Tm^3 fiber laser pump diodes to the final total supercontinuum output is ~ 3.3%, which is comparable to recent results of 2 μm pumped SC [23],[33]. The current arrangement exhibits a reduced complexity compared to multi-stage amplifier systems.

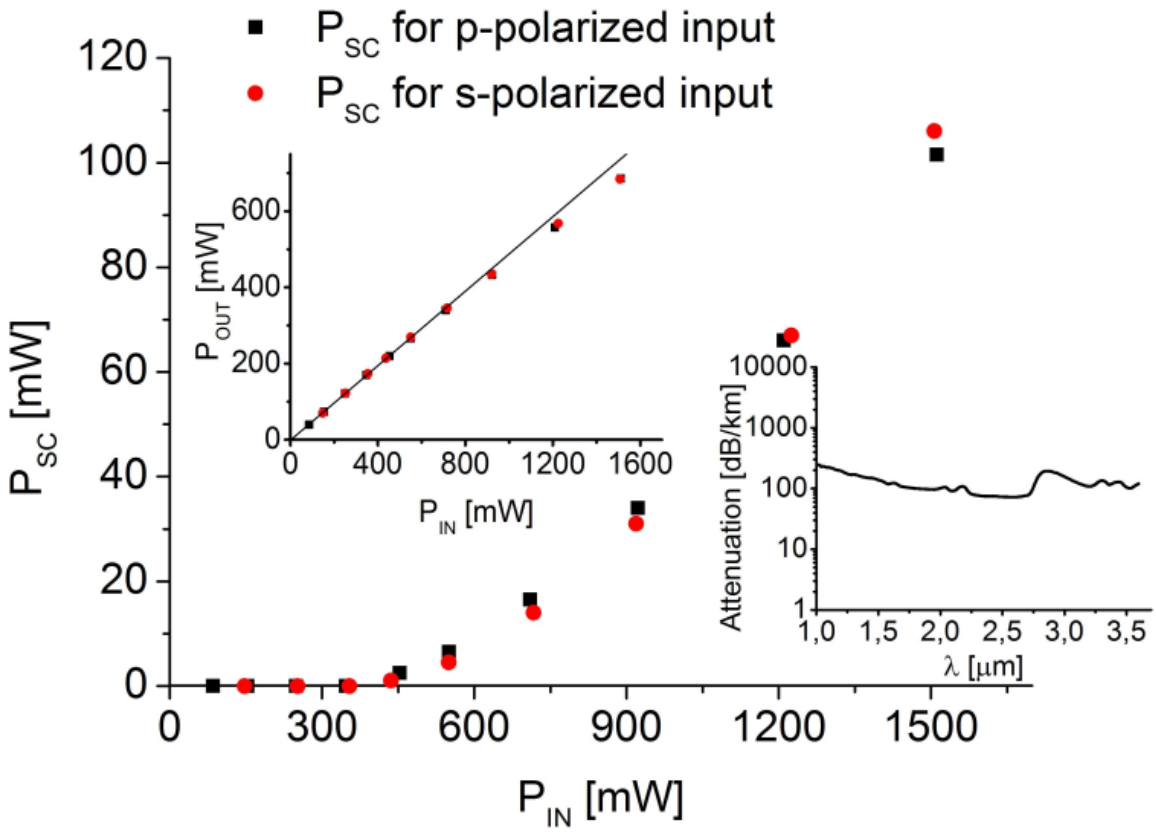

Figure 4-19: Power Shifted Beyond 2340 nm for Different Average Pump Powers. The upper inset shows for comparison the overall average output power (the black line being a linear interpolation of the first five points). The second inset shows the passive attenuation of the ZBLAN fiber.

The SC generated in this work is comparable to the spectra presented by other 2 μm pumped SC experiments [23] regarding the power drop from peak spectral pump power to SC plateau and the negligible amount of spectral power that is shifted to short wavelengths below the pump wavelength.

In conclusion, a simultaneous actively Q-switched and actively mode-locked Tm^{3+} fiber laser with up to 5 W of average output power at ~ 60 kHz Q-switch envelope repetition rate was presented. Up to ~ 8 μJ sub-pulses with peak powers reaching 2.4 kW were generated. Using this laser as a pump source for SC generation in a ZBLAN fiber over 1080 mW of supercontinuum from 1.9 μm to beyond 3.6 μm was obtained. The overall efficiency with respect to the diode pump power of the total laser set-up was 3.3%. The scalability of the pump laser (not average power limited) makes this scheme promising for future high-average-power SC sources with reduced complexity due to the single-oscillator approach.

4.2.2 Supercontinuum Generation in Chalcogenide Fibers

Contributors to this section: Rafael R. Gattass[9], L. Brandon Shaw[9], Vinh Q. Nguyen[9], Paul C. Pureza[9], Ishwar D. Aggarwal[10], Jasbinder S. Sanghera[9]

From: Optical Fiber Technology, 18, pp. 345-348 (2012)

[9] U.S. Naval Research Laboratory, 4555 Overlook Avenue SW, Washington, DC 20375-5338, United States.
[10] Sotera Defense Solutions, 2200 Defense Highway, Crofton, MD 21114, United States.

In this section we present an all-fiber based supercontinuum source with emission covering the wavelength range of 1.9 – 4.8 µm is demonstrated. The laser source is based on a combination of silica Commercial-Off-The-Shelf (COTS) components and a chalcogenide-based non-linear optical fiber. The system provides 10 dB spectral flatness from 2.0 µm to 4.6 µm, and 20 dBm points from 1.9 µm to 4.8 µm. The output power is 565 mW, but scalable by scaling the repetition rate. The limit on the long-wavelength edge of the system is identified as an extrinsic absorption feature in the fiber used; confirming the system could be scaled to generate a broadband source even further in the infrared.

There have been several demonstrations of mid-infrared supercontinuum generation with optical fibers [9],[15],[20]-[23],[53]-[56]. Chalcogenide fibers (fibers based on chalcogen elements S, Se and Te) are natural candidates for infrared supercontinuum sources due to their long-wavelength multi-photon absorption edge. For example, the multi-photon absorption edge for an As_2S_3 is 7.4 µm [19], and can be even further for Se-based and Te-based chalcogenide fibers. For applications involving non-linear optical processes, chalcogenide fibers are even more suitable [19] given their high non-linear refractive index n_2 (~ 5 x $n_2^{tellurite}$, ~ 500 x n_2^{silica} and ~ 1000 x $n_2^{fluoride}$) [55] and high peak Raman gain g_r (~ 65 x g_r^{silica} [57],[58], ~ 46 x $g_r^{fluoride}$ [59], ~ 2 x $g_r^{tellurite}$ [60]). In addition, chalcogenides have high optical damage threshold (e.g. > 25 GW/cm^2 at 2.4 µm for As_2S_3 [54]) and environmental stability (e.g. non-hydroscopic for most chalcogenide glasses including As_2S_3, As_2Se_3). It is the combination of wide transmission range, strong non-linear properties, high optical damage threshold and environmental stability that make chalcogenide fibers an ideal system from fiber-based supercontinuum laser sources. The first mid-infrared fiber supercontinuum source was demonstrated using chalcogenide fibers in 2005 [53],[61], but was based on an optical parametric amplifier pumped by a Ti:sapphire laser. The supercontinuum source was limited in spectral range (2 – 3.5 µm) and average power (< 10 mW). In [54] we transitioned to a fiber-based pump source which still emitted close to 2.5 µm, increasing the average power (140 mW) and extending the spectral range to cover from 1.5 to 4.8 µm. The supercontinuum laser system was based on a custom picosecond mode-locked laser seed system [62], amplified in a Er-doped fiber amplification stage, soliton-self frequency shifted to 2 µm and further amplified in a Tm-doped fiber amplification stage. In this paper, we transition to an all COTS-based laser system still using a chalcogenide fiber in the last stage for high non-linear mid-infrared supercontinuum source.

4.2.2.1 Experimental Set-Up

Figure 4-20 shows a schematic of the laser system developed for the supercontinuum source. Multi-stage master oscillator power amplifier geometry is used following a similar approach as the one described in [63]. A 40-ps, 10-MHz Er-fiber-based laser with 200 mW average output power was sourced from a commercial vendor and is used as a seed for the system. The use of a picosecond pulse duration seed minimizes the effect of Brillouin scattering as power is increased while being fairly insensitive to dispersion. Spectral filtering with narrow band filters and temporal filtering with an acousto-optic modulator are done to the output of the seed laser to reduce power carried by amplified spontaneous emission to 30 dB of the peak wavelength. The seed is amplified in multiple stages, and the power is soliton shifted into the Tm amplification band. Because the soliton shifting occurs in a non-Tm-doped fiber, no amplified spontaneous emission is present in the emission band of Tm and the soliton-shifted pulses act as a new background free “seed” for the Tm amplification. Propagation in a highly non-linear fiber continues to shifts the center wavelength further into the infrared. The chalcogenide fiber used in the last stage is a step-index core-clad As_2S_3 fiber with a 10 µm core diameter and numerical aperture of 0.3 and 2 m length. The step-index fiber was fabricated through a double crucible process and has a minimum transmission loss of 0.7 dB/m at 1.5 µm. The end faces of the fiber are cleaved and mechanically coupled to the silica without any patterning or treatment resulting in a total 68% reflection loss from both end faces.

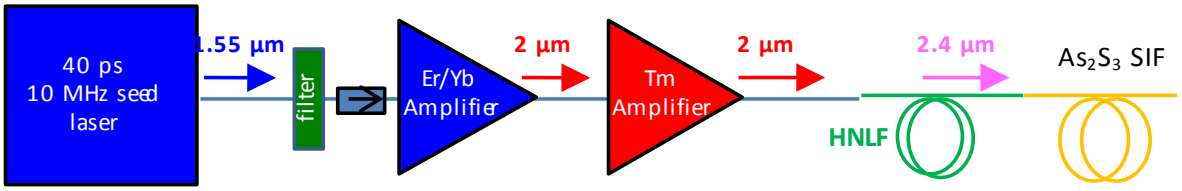

**Figure 4-20: Schematic of All Fiber Laser System.
HNLF: Highly Non-Linear Fiber; SIF: Step Index Fiber.**

4.2.2.2 Results

The laser system was characterized before and after the insertion of the chalcogenide fiber in the system. The optical beam's wavelength prior to entering the chalcogenide fiber is centered around 2.45 µm and has approximately 100 nm bandwidth. At this stage, the output is approximately 1.4 W of average power. After propagating through the As_2S_3 chalcogenide fiber, 565 mW broadband supercontinuum is observed.

Figure 4-21 shows the generated supercontinuum spectrum. The spectrum is measured with a scanning monochromator and three-stage thermo-electrically cooled HgCdTe detector. Higher order diffraction orders are removed by a series of longpass filters.

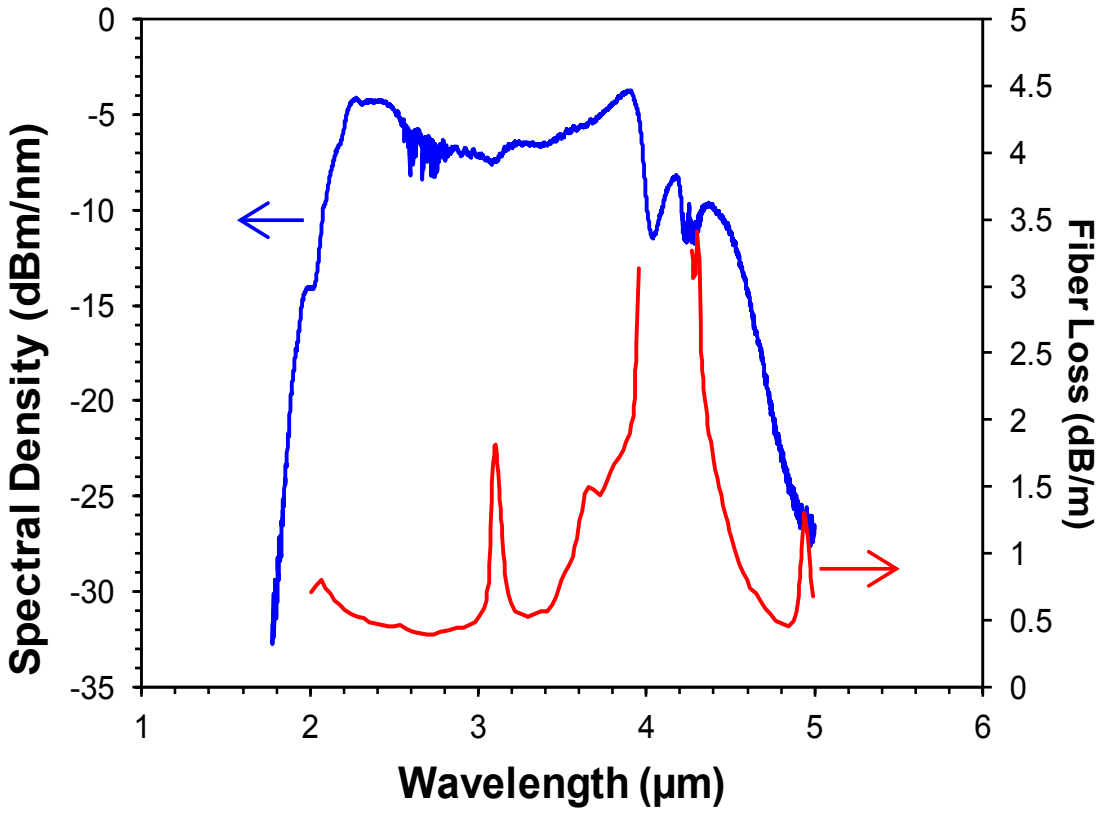

Figure 4-21: Supercontinuum Spectrum (Blue Curve) and Estimated Loss Curve for Chalcogenide Fiber (Red Curve).

The spectrum, at the 20 dBm points, spans from 1.9 µm to 4.8 µm. The noise observed around 2.8 µm is due to atmospheric absorption bands caused by the use of a non-purged monochromator system. The system

provides 10 dB spectral flatness over 2.0 – 4.6 µm. We have measured the beam profile for the output beam at 2.2 µm with an infrared camera. Although the fiber supports a low number of modes, the system is aligned to excite only the lowest order mode at this wavelength. Given the fiber numerical aperture and core diameter, as the supercontinuum continues to broaden, the fiber becomes single mode at approximately 3.8 µm. Although we have not been able to measure the mode between 2.2 and 3.8 µm, we believe the short length of fiber used and the efficient energy transfer indicates that the beam remains single mode over all the emission wavelengths. The laser system was tested over a period of approximately one month. Average power and spectrum broadening were monitored weekly and remained repeatable over the whole monitoring time. Detailed characterization of noise and further long-term stability by a NIST-calibrated sensor system is currently underway. Figure 4-22 shows the evolution of the supercontinuum spectrum with respect to increase pump power. As can be seen the spectrum broadens mostly to longer infrared wavelengths with increasing pump power. The supercontinuum spectrum seems to be attenuated at the same location as a known impurity band (shown in Figure 4-21), although some power is still observed beyond the impurity band.

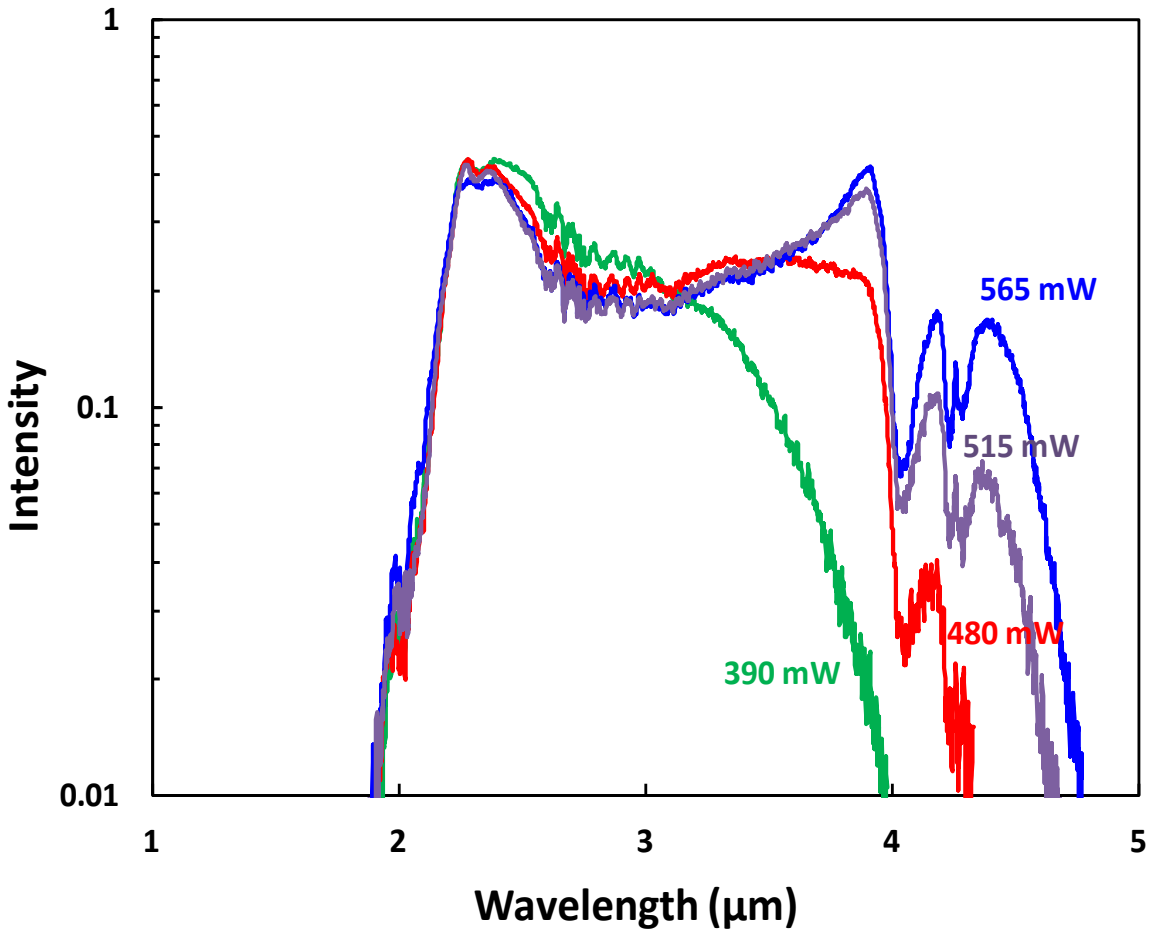

Figure 4-22: Spectral Evolution of Supercontinuum Source as a Function of Measured Output Power.

4.2.2.3 Discussion

Previous demonstrations of MIR supercontinuum generation in other materials systems used anomalous dispersion pumping for supercontinuum generation [6],[19],[55]. Here, normal dispersion pumping is

utilized for supercontinuum generation. The process of supercontinuum generation in a normal dispersion fiber is known and is primarily interplay between stimulated Raman scattering and self and cross-phase modulation [63]. We speculate that given the asymmetric power induced broadening towards infrared wavelength, the bandwidth of the laser beam before entering the chalcogenide fiber (100 nm) and the bandwidth of the Raman gain in As_2S_3 fiber (85 cm^{-1}) [59], the observed spectrum can be attributed to about 6 or 7 stokes shifts, with spectral broadening at each shift caused by a convolution of the Raman gain spectrum with the broadband pulse out of the silica stage as well as smoothing from self-phase modulation and cross-phase modulation.

While a photonic crystal design to enable anomalous dispersion pumping could have been used in the system [20], photonic crystal fibers designs to shift the zero dispersion wavelengths in As_2S_3 result in small core fiber diameters which can be difficult to fabricate and typically have higher transmission losses as well as high insertion losses. Power scaling with such small core structures is also problematic, especially with suspended core microstructured fiber where the core is effectively thermally isolated from the cladding by an air layer. The use of normal dispersion pumping in step index fiber was chosen instead of a photonic crystal fiber design to allow for increased power handling and future power scaling. The transmission range of As_2S_3 fiber extends further out than the maximum wavelength observed in the supercontinuum spectrum of Figure 4-21. The drop in power around 4.1 µm is not due to an intrinsic limit in the material system, but instead to an extrinsic impurity present in the fiber. Overlaid in Figure 4-21 is the measured fiber loss for a multi-mode fiber batched under similar processing conditions as the 10 µm core fiber used in this experiment. The large absorption peak around 4.1 µm is due to ppm-level hydrogen impurities, which bond to form H-S in the fiber. Because the supercontinuum process involves broadening the spectrum from shorter wavelengths, the H-S absorption band attenuates the power and halts the broadening. Given the width of the absorption band and the bandwidth of the Raman cross-section in As_2S_3, theoretically if there is enough power present below the absorption peak, a Raman scattering event could leap enough energy over the absorption band and continue broadening the supercontinuum even further. The power dependent “hop” over the absorption band is clearly seen in the power evolution of the supercontinuum shown in Figure 4-22. The spectrum broadens towards longer wavelengths with increasing pump power. At the low end, output power level of 390 mW, spectral broadening has not yet reached the impurity band. At 480 mW output power, there is not enough power in the fiber to induce enough non-linearity to hop over the absorption band and spectrum broadening stops at about 4 µm. As the pump power is further increased (515 mW output power), a peak beyond 4.1 µm is visible with enough power to continue broadening towards longer wavelengths. Even further increase in pump power is one alternative for broader sources, but the same effect could be accomplished by reducing the losses due to the impurity band. There are known processes for reducing the level of impurities in chalcogenide fibers with attenuations of less than 3 dB/m at 4.0 µm already demonstrated [64]. A combination of increased power and better purification should significantly improve the bandwidth of the supercontinuum. Besides improvements to the bandwidth of the system, the fiber-based architecture used in this experiment can be scalable to higher average powers. Two common approaches can be used for power scaling: increasing repetition rate while maintaining peak power (as done in [33]); and increasing peak power per pulse while maintaining repetition rate.

For the first approach, the current system is limited to 10 MHz by one of the time-filters being used, but there are other commercial alternatives up to 100s of MHz. The repetition rate could be scaled up while maintaining the peak power constant, thereby reducing the risk of optical damage.

In the second approach, the peak power per pulse can be increased, resulting in scaling of the average power. In the system presented here, we have been limited to the maximum pump power. However, because the current supercontinuum scheme operates in the normal dispersion regime of the fiber, the core size of the fiber can be increased while maintaining intensity in the core of the fiber to scale to higher powers.

We have used a combination of both approaches to scale the peak power from our preliminary results of 140 mW [54] to 565 mW. Previously, the pump source operated at 560 kHz with a peak power per pulse

> 10 kW. Our power scaled supercontinuum pump source operates at a 10 MHz repetition rate with a peak power per pulse of 3.5 kW. By operating the system with the peak power of the first demonstration (10 kW) and the repetition rate of the second system (10 MHz), we project a scaled average power between 1.5 and 2.5 W.

A limitation to power scaling through repetition rate scaling would be reaching the damage threshold for the fiber. However for our pulse width of less than 100 ps and an incident pump far from the two-photon absorption edge (as in our case with a pump around 2.45 µm), we observe the peak intensity damage threshold to be very high. For example, for the system described in this paper, the incident peak intensity at the fiber front face is approximately 4.5 GW/cm^2, while a previous interaction of this system with a lower repetition rate lead to an incident peak intensity of approximately 12 GW/cm^2 [54]. The scalable fiber-based mid-infrared supercontinuum source demonstrated in this section addresses immediate needs for infrared sources in metrology such as the one for the Hyperspectral Image Projector (HIP) being developed at National Institute of Standards and Technology [65]-[67]. Requirements for illumination of the HIP system are spectral power density of 10 dBm/nm or higher, spectral flatness of 10 dB within the band of interest (3 – 5 µm) and continuous wave or high repetition rate pulse trains with rates much faster than the temporal response of the system under test (typically 1 MHz or better repetition rate). The output diameter of the fiber can be no greater than 20 µm in diameter to maintain spectral resolution of the system. Currently, we are power scaling and packaging the supercontinuum source for implementation in the HIP.

In conclusion, we presented in this section an all-fiber chalcogenide-based supercontinuum source with emission covering the wavelength range of 1.9 – 4.8 µm. The system architecture is based on a combination of silica commercial-off-the-shelf components and an As_2S_3 step index non-linear optical fiber. The supercontinuum spectrum has 10 dB spectral flatness from 2.0 µm to 4.6 µm, 20 dBm points from 1.9 µm to 4.8 µm, with a total output power of 0.565 W. We identify the current long-wavelength limit of the system to be due to an extrinsic absorption in the fiber, acknowledging further broadening is still possible in this glass system.

4.2.3 Supercontinuum Generation in Fluoroindate Fibers

4.2.3.1 Supercontinuum Generation in Fluoroindate Fiber with Ultrashort Laser Pulses

Contributors to this section: Francis Théberge[11], Jean-François Daigle[11], Denis Vincent[11], Pierre Mathieu[11], Jean Fortin[11], Bruno E. Schmidt[12], Nicolas Thiré[12], François Légaré[12]

In this section we present the first demonstration of SC generation in a fluoroindate based single-mode fiber. These fibers exhibit a minimal loss of 0.1 dB/m at 3.2 µm and a loss inferior to 0.8 dB/m at 5 µm. With this fiber, we demonstrated the generation of 20 dB spectral flatness SC spanning from 2.7 µm to 4.7 µm.

The attenuation spectrum for the single-mode fluoroindate based fiber is presented in Figure 4-23 (black line). For comparison, Figure 4-23 presents also the attenuation spectrum for a single-mode fluorozirconate based fiber having similar core diameter. In this section, we compare the SC generation in these two fibers and their specifications are listed in Table 4-5. The fluoroindate fiber has been produced by Le Verre Fluoré and its glass composition is similar to Ref. [69].

[11] DRDC Valcartier, 2459 route de la Bravoure, Québec (Québec) G3J 1X5, Canada.

[12] INRS-EMT, 1650 Lionel-Boulet Blvd, Varennes (Québec) J3X 1S2, Canada.

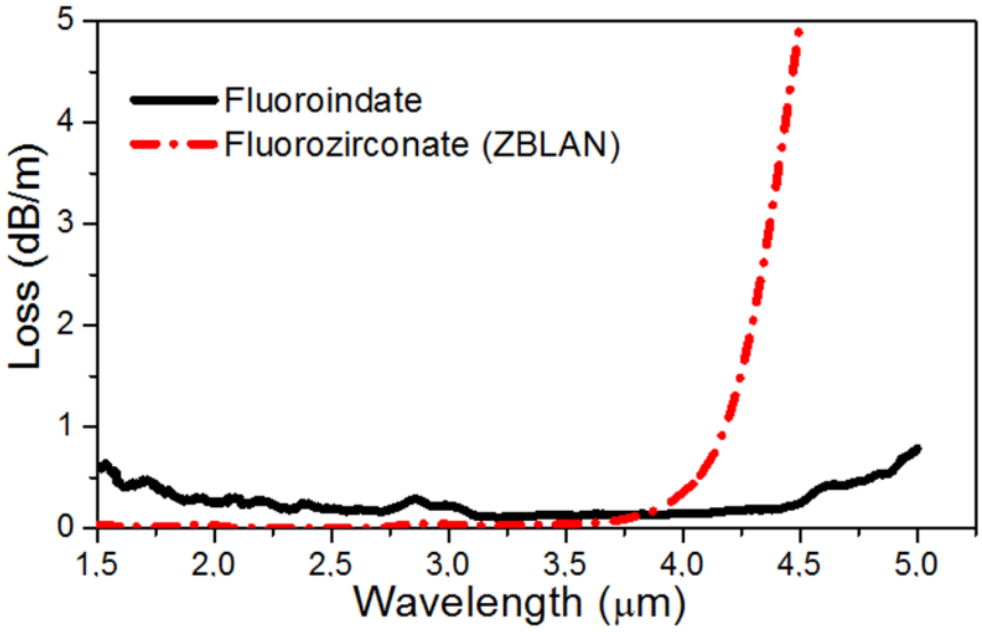

Figure 4-23: Attenuation Spectrum of the Fluoroindate-Based Fiber (Black Line) and ZBLAN Fiber (Red Dash-Dot).

Table 4-5: Parameters of Fluoride Fibers.

Fiber	Fluoroindate	ZBLAN
Core Diameter	16 μm	16 μm
Cladding Diameter	120 μm	125 μm
Numerical Aperture	0.14	0.19
Cut-Off Wavelength	2.8 μm	4.2 μm
Zero Dispersion	1.83 μm	1.63 μm
Length	9.5 m	9.0 m

The fibers described in Table 4-5 have a relatively large core diameter for SC generation applications enabling these fibers to sustain high average laser powers. Various laser pulse parameters have been injected into these fibers with pulse durations ranging from 70 fs to 20 ns and with central wavelength between 1.5 μm and 3.4 μm. For the fluoroindate based fiber, more than 12 W of average power centered at 1.5 μm and with peak power exceeding 10 kW (20 ns pulsewidth) can be injected into the fiber core without any damage, which makes this fiber interesting for multi-watt SC sources.

In order to achieve significant broadening, the zero Group Velocity Dispersion (GVD) of the fiber should be close to the center wavelength of the laser pulse used for SC generation, with the laser wavelength slightly shifted towards the anomalous GVD regime. This minimizes the walk-off between the different regions of the generated spectrum, allowing for further spectral broadening [38]. The zero GVD wavelength of the fluoroindate-based fiber is 1.83 μm, but more interesting is the very small dispersion variation beyond the zero GVD wavelength from 1.8 μm to 4 μm with a value inferior to 10 ps/km•nm around 3 μm [69]. Therefore, the central wavelength of the laser pulse injected into the fiber can be tuned over a wide spectral range without undergoing severe temporal broadening due to large anomalous GVD.

In order to investigate the SC generation, different pulse duration at different center wavelengths were coupled into the fluoroindate fiber. The experiments were performed using the infrared beam line at the Advanced Laser Light Source (ALLS) [70]. An optical parametric amplifier pumped by a Titanium-sapphire allows the generation of wavelength-tunable laser pulses in the range of wavelength between 1.4 µm to 4 µm. For wavelengths between 1.4 µm to 2 µm, different transform limited pulse duration from 70 fs up to 850 fs were achieved through spectral filtering by closing a variable slit in the Fourier plane of a 4-f set-up. At longer wavelengths up to 4 µm, narrow band-pass filters were used for this purpose.

Both fiber ends were cleaved by a diamond stylus to ensure a sufficiently flat interface. The generated and transmitted SC was measured by an $f = 12.5$ cm monochromator equipped with a 300 lines/mm diffraction grating and a PbSe detector, giving a spectral resolution around 5 nm. In order to block any second diffraction order of the grating overlapping with the SC spectrum, a Germanium window was used in front of the detector to record the spectrum from 1.9 µm up to 3.5 µm. To record the spectrum from 3 µm up to 5.5 µm, a long-wavelength pass filter transmitting above 3 µm was used in front of the detector.

Figure 4-24 presents the generated SC in the fluoroindate and the ZBLAN fibers, when 70 fs, 3.4 µm laser pulses were injected in these fibers. Figure 4-24(a) presents the spectral broadening into the 9.5-m long single-mode fluoroindate based fiber. We observe the continuous broadening as we increased the laser pulse energy injected into the fiber. For the lowest pulse energies, the spectral broadening is asymmetric and occurs mainly towards the longer wavelength due to the self-phase modulation occurring in anomalous dispersion regime. For a laser pulse energy of 120 nJ injected into the fiber, the peak power of the laser was 1.7 MW. Such peak power is about 20 times lower than the critical power for self-focusing (Pcr ≅ 39 MW) in fluoride glasses [28],[68]. At 120 nJ per pulse, the SC produced in the fluoroindate fiber provides 20 dB spectral flatness from 2.7 µm to 4.7 µm.

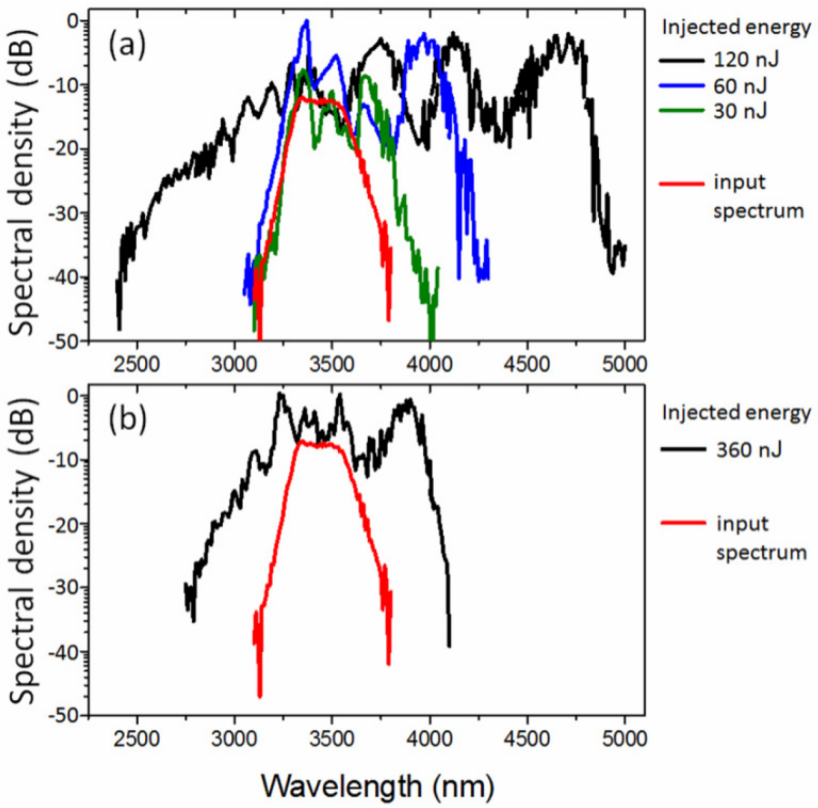

Figure 4-24: (a) Spectral Evolution of Supercontinuum as a Function of Measured Energy per Pulse Injected in Fluoroindate-Fiber; (b) Supercontinuum Generation in ZBLAN Fiber.

During SC generation, self-phase modulation and four-wave mixing induce initially the spectral broadening before higher order dispersion causes fission of the laser pulse. After the fission of the laser pulse into multiple solitons, the individual solitons redshift by the Raman self-frequency shift effect and emit phase-matched dispersive waves at wavelengths shorter than the zero GVD [39].

The spectral modulations observed in the SC of Figure 4-24(a) are partly attributed to the spectral interference resulting from the spectral broadening and phase-shift induced by the self-phase modulation. The stronger spectral modulations for the red-shifted part of the SC are probably enhanced by the generation of self-frequency shift Raman solitons [39],[71]. In Figure 4-24(b), it is interesting to compare the SC generation in ZBLAN. Because the dispersion in ZBLAN is 2 – 3 times larger at 3.4 µm than for the fluoroindate fiber, more energetic laser pulses have to be injected into the ZBLAN core in order to preserve similar soliton order $N \cong 7$ for the maximum pulse energy injected in both fibers. For the ZBLAN fiber, SC generation could not expand beyond 4.1 µm because of the important absorption beginning around 4 µm (see Figure 4-23). On the other hand, the blue-shifted extension of the SC in ZBLAN is weaker because the ZBLAN dispersion is larger and induces the lengthening of the laser pulses at shorter distance into the fiber [68]. The 20 dB spectral flatness in ZBLAN spans from 2.9 µm to 4.0 µm which is two times narrower than for the fluoroindate fiber.

The absorption edge in fluoroindate was not the dominant factor limiting the SC expansion observed in Figure 4-24(a), because we did not observe a decrease of the SC as sharp as in Figure 4-23(b) and the attenuation was only 0.5 dB/m in the fluoroindate fiber around 4.7 µm. In fact, the SC extension in the fluoroindate fiber was probably limited by the dispersion of the very broad SC laser pulse generated into the fluoroindate fiber.

Usually the maximum spectral broadening of the laser pulse is achieved for the distance at which soliton fission occurs. Optimizing the fiber length just shorter than this point is the basis of the higher-order soliton effect compression technique, and a number of empirical expressions for this characteristic distance have been developed [38]. It is particularly useful to refer to this distance as the fission length (L_{fiss}), written in the simplified form:

$$L_{fiss} = \sqrt{L_D L_N}$$

where $L_D = {\tau_0^2}/{|\beta_2|}$ is the dispersion length, $L_N = {(cA_{eff})}/{(n_2 \omega_0 P_0)}$ is the non-linear length, τ_0 is the initial pulsewidth, β_2 is the group velocity dispersion, c is the light speed, A_{eff} is the effective core area, n_2 is the non-linear index of refraction, ω_0 is the central frequency, and P_0 is the initial peak power. According to the initial laser parameters, the fiber core diameter and the fluoroindate dispersion of 10 ps/km•nm around 3.4 µm, we obtain a fission length $L_{fiss} \approx$ 2 cm. Also, when estimating the soliton order (N) for the 120 nJ laser pulse injected into the fluoroindate fiber, we obtain a relatively low order:

$$N = \sqrt{\frac{L_D}{L_N}} \cong 7$$

which indicates that the fission did not occur randomly due to modulation instability and the coherence of the laser pulse was preserved during the SC generation [6].

Considering the fluoroindate fiber dispersion, the 70 fs initial laser pulse duration and the few centimeters long fission length, we determined that most of the spectral broadening from self-phase modulation and Raman-shift occurred within the first tens of centimeters of the fiber. Thereafter, the dispersion lengthened the broadband laser pulsewidth and decreased significantly the peak intensities. Finally, linear propagation of the generated SC occurred for the rest of the fiber length (or approximately for 8.5 m of propagation). At the

fluoroindate fiber output, the pulse duration of the chirped SC laser pulse is estimated to be ~ 100 ps and its peak power is ~ 1 kW. These estimations and the SC presented in Figure 4-24(a) point out the very good transmission of the fluoroindate fiber for the whole SC generated at the beginning of the fiber because no absorption bands or absorption cut-off were observed in the measured output spectra.

In summary, the anomalous dispersion of step-index fluoroindate fiber in the mid-infrared is relatively low and permits the SC generation from a wider range of initial central wavelength for the injected laser pulses. Moreover, the very low loss between 1 µm and 5 µm allows a continuous expansion of the SC without any interception from an absorption edge or an absorption band as in the case of long ZBLAN or long chalcogenide fibers, respectively. With a large core single-mode fluoroindate fiber, we demonstrated the generation of 20 dB spectral flatness SC from 2.7 µm to 4.7 µm, which covers almost entirely the mid-infrared atmospheric windows. Single-mode fluoroindate fiber represents unambiguously a promising fiber for the generation of multi-watt SC over a wide spectral range.

4.2.3.2 High Average Power Supercontinuum Generation in an Indium Fluoride Fiber

Contributors to this Section: Jacek Swiderski[13], Francis Théberge[14], Maria Michalska[13], Pierre Mathieu[14], Denis Vincent[14]

In this section we report the first demonstration of Watt-level Supercontinuum (SC) generation in a step index indium fluoride (fluoroindate) fiber pumped by a 1.55 µm fiber Master-Oscillator Power Amplifier (MOPA) system. The SC is generated in two steps: first ~ 1 ns amplified laser diode pulses are broken up into soliton-like sub-pulses leading to initial spectrum extension and then launched into a fluoride fiber to obtain further spectral broadening. The pump MOPA system can operate at a changeable repetition frequency delivering up to 19.2 W of average power at 2 MHz. When the 8-m long fluoroindate fiber was pumped with 7.54 W at 420 kHz output average SC power as high as 2.09 W with 27.8% of slope efficiency was recorded. The achieved SC spectrum spread from 1 to 3.05 µm.

To extend the transmission range in the mid-IR while providing the high-power capacity at the same time, indium fluoride (fluoroindate) fibers seem to be a good choice. They have lower phonon energy than ZBLAN glasses which increases their transparency in the mid-IR region to ~ 5.5 µm [72]. Furthermore, to obtain SC generation, they can be pumped effectively by the novel pulsed laser system already developed, for example [14],[16],[36],[50],[73]-[74]. Even though fluoroindate fibers (and suitable pump sources) are accessible, there have been no reports on high-power SC generation in these media.

The experimental arrangement for SC generation is shown in Figure 4-25. Basically it consists of two parts – a pump laser (developed at MUT, Poland) and a non-linear fluoride fiber (provided by DRDC, Canada). The pump MOPA system is a four-stage fiber amplifier, seeded with a directly modulated Distributed Feedback (DFB) laser delivering 1 ns pulses at λ = 1.55 µm and at variable Pulse Repetition Frequency (PRF) in the range of 0.2 – 2 MHz.

[13] Institute of Optoelectronics, Military University of Technology, 2 Kaliskiego Street, 00-908 Warsaw, Poland.

[14] DRDC Valcartier, 2459 route de la Bravoure, Québec (Québec) G3J 1X5, Canada.

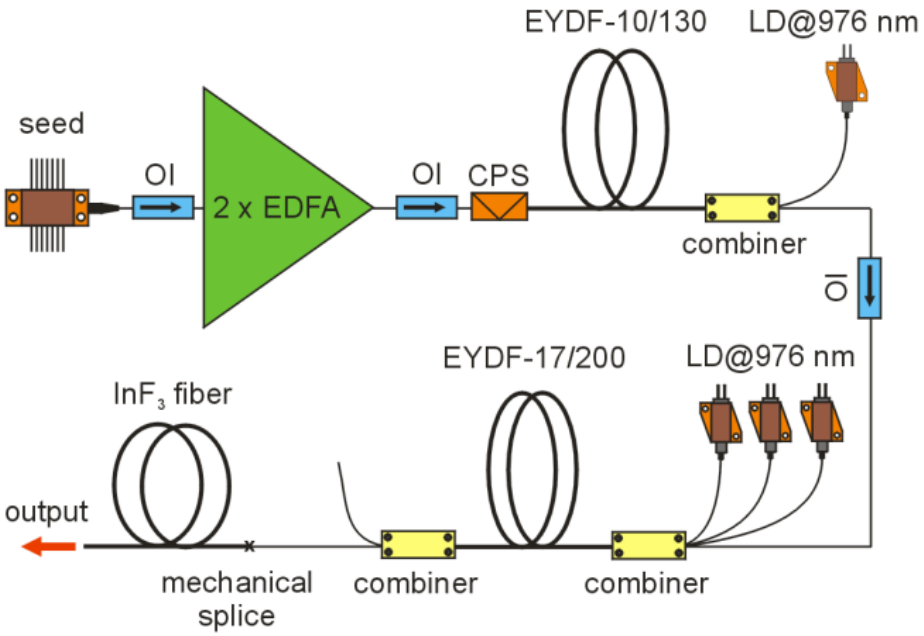

Figure 4-25: Set-Up for SC Generation. OI – Optical Isolator; EDFA – Erbium-Doped Fiber Amplifier; EYDF – Erbium:Ytterbium-Doped Fiber; CPS – Cladding Power Stripper; LD – Laser Diode.

The optical pulses delivered by the seed diode are first pre-amplified in two core-pumped Er-Doped Fiber Amplifiers (EDFAs) and one cladding pumped Er:Yb-Doped Fiber mid-Amplifier (EYDFA1). This system part could generate up to 2.1 W of average output power providing up to 58.5 dB of total gain, as reported in [2],[74]. The pulse train from the EYDFA1, after optical isolation, is then boosted in an Er:Yb-Doped Fiber power Amplifier (EYDFA2). The gain medium of EYDFA2 is a ~ 4.5-m long Er^{3+}:Yb^{3+}-co-doped, polarization maintaining, double-clad, Large-Mode-Area (LMA) fiber (EYDF) with a core diameter of 17 µm and a clad diameter of 200 µm, the NA was 0.17 for the core and 0.46 for the inner clad. A (6 + 1) x 1 pump combiner with a signal feedthrough (signal input: SMF-28; pump ports: 105/125 µm, 0.22 NA; signal output: passive double-clad 17/200 µm fiber, 0.17/0.46 NA) was used to deliver pump radiation to the active fiber. It combined power emitted by three 30 W multi-mode fiber-pigtailed (core diameter of 105 µm) laser diodes operating at the central wavelength of λ = 976 nm. Over 90% of the launched pump light was absorbed in the active fiber. The output of the LMA EYDF was first equipped with a home-made mode field adaptor (fiber taper) with a 17/200 µm (0.1/046 NA) fiber at the input and 25/300 µm (0.1/046 NA) fiber at the output. Then it was fusion spliced to a second pump combiner (signal input: passive double-clad 25/300 µm fiber, 0.1/0.46 NA; pump ports: 105/125 µm, 0.22 NA; signal output SMF-28) providing > 85% signal transmission. This allowed for filtering the unabsorbed pump power at λ = 976 nm from the amplified 1.55 µm pulse train. Furthermore, the 1.5-m long output pigtail fiber of the second combiner with ~ 8 µm core diameter permitted easy pump light coupling into the non-linear fiber. The active fiber of the EYDFA2 was coiled on a 10-cm diameter cylinder placed on a water-cooled heat-sink that was kept at 18 – 19 °C. Finally, the output signal fiber port of the combiner was mechanically spliced to the input end of the fluoroindate fiber with over 90% launching efficiency. Both fibers ends were angle-cleaved to prevent any reflection in the system.

Figure 4-26 presents the MOPA system average output power (after the 1.5-m long SMF fiber), for the PRF of 0.42, 1, and 2 MHz versus absorbed pump power in the EYDFA2. The inset in the top-left corner presents the spectrum generated at the system output for 2 MHz repetition rate and 19.2 W of output power while the inset in bottom right corner depicts the spectrum measured for 0.42 MHz repetition rate and 7.54 W of output power.

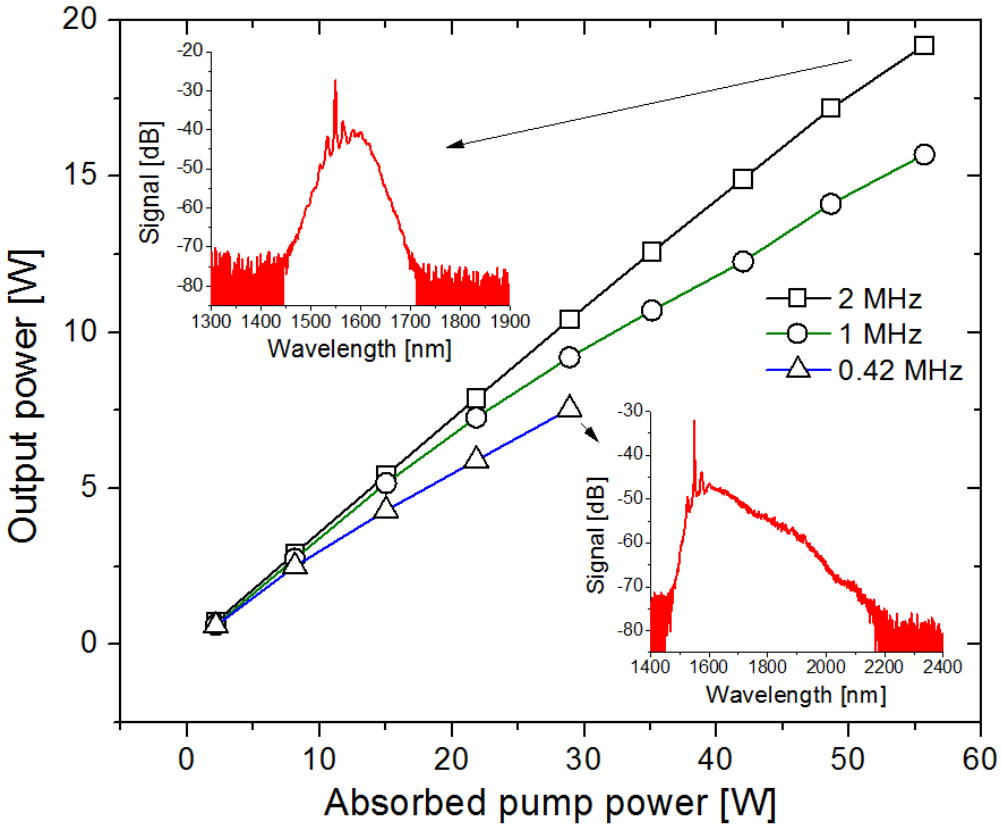

Figure 4-26: The Pump MOPA System Output Power. Top inset – Signal spectrum at 2 MHz and 19.2 W of output power; Bottom inset – Signal spectrum at 0.42 MHz and 7.54 W of output power.

As can be seen in Figure 4-26, average output power increases almost linearly with the rise of absorbed pump power. The maximum average output power for 55.7 W of absorbed pump power, measured at the highest PRF, was 19.2 W with 35% of slope efficiency determined with respect to absorbed pump power. For the lowest applied repetition rate of 0.42 MHz and 29 W of absorbed pump power, the output power was measured to be 7.54 W with 26% slope efficiency. The limit of output power for the lower PRF resulted from the presence of Amplified Spontaneous Emission (ASE) emitted by the Yb^3-dopant of the gain fiber. With the increase in pump power, the output spectrum gradually extended towards mainly mid-IR region. For instance, at 420 kHz repetition rate and output power of 7.54 W the spectrum covered the band of ~ 1.45 – 2.15 μm. The shape of the spectra presented in the insets is typical for pumping in the anomalous dispersion region of the fiber – with signature of a residual peak at the pump wavelength and a continuum signal spread about 15 – 20 dB below the maximum peak. Furthermore, the spectra show a set of two sidebands, symmetrically separated from the pump wavelength. It is a characteristic feature for Modulation Instability (MI) phenomenon which causes the breakup of 1 ns pulses in the 1.5-m long SMF into femtosecond pulses [16] leading to boosting pulse peak power and thus spectrum extension.

In the next step, the pump pulse train with an initially broadened spectrum was launched into the 8-m long fluoroindate fiber with a core/clad diameter of 16.7/125 μm and a core NA of 0.17. Its attenuation curve is shown in Figure 4-27. The losses in the range of 1.5 – 5 μm were measured to be < 0.8 dB/m. The minimum losses of 0.3 dB corresponded to $\lambda = 4.15$ μm. The peak at ~ 2.9 μm is related to OH absorption. The Zero Dispersion Wavelength (ZDW) of the fiber was at 1.83 μm, as specified by the manufacturer. The cut-off wavelength was measured to be at 3.72 μm, which means that the fiber is multi-mode at the pump wavelength and single-mode for $\lambda > 3.72$ μm.

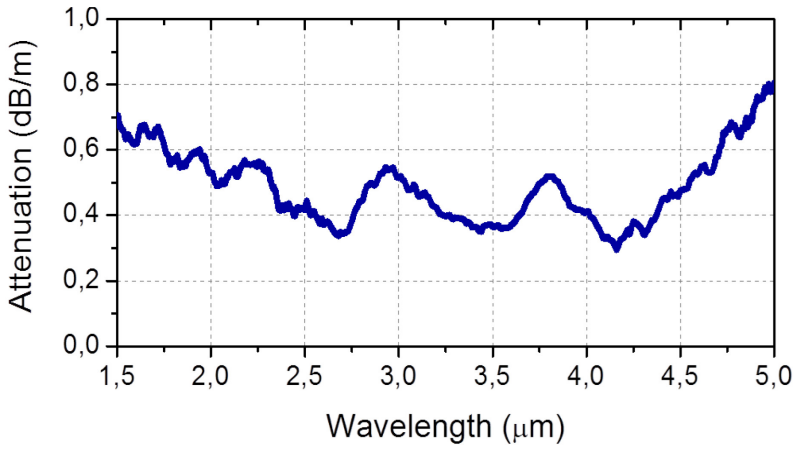

Figure 4-27: Attenuation Curve of the Fluoroindate Fiber.

During the experiment we decided not to exceed 8 W of pump power at 1.55 μm launched into the non-linear fiber, which we considered to be safe for it. To determine the best conditions for SC generation we changed the PRF of the MOPA system from 2 MHz to 0.4 MHz while keeping its output power constant and monitoring a spectrum at the fluoride fiber output end. Best continua extension was achieved at lower repetition rates (< 500 kHz) which can be attributed to the boost of peak power launched into the 1.5-m long SMF and then into the fluoride fiber. It leads to the enhancement of non-linearity and thus efficiency of SC generation process. Pumping the fluoroindate fiber with 7.54 W at 0.42 MHz repetition rate we achieved 2.09 W of total average output SC power, of which 0.96 W (45.9%), 0.57 W (27.3%) and 177 mW (8.5%) corresponded to wavelengths longer than 1.65 μm, 2 μm, and 2.4 μm, respectively (Figure 4-28). In the present MOPA system configuration it was difficult to lower the PRF below 400 kHz while keeping the output power at > 5 W, which resulted from the presence of ASE at ~ 1.06 μm coming from the EYDFA2, affecting the whole system performance at lower repetition rates.

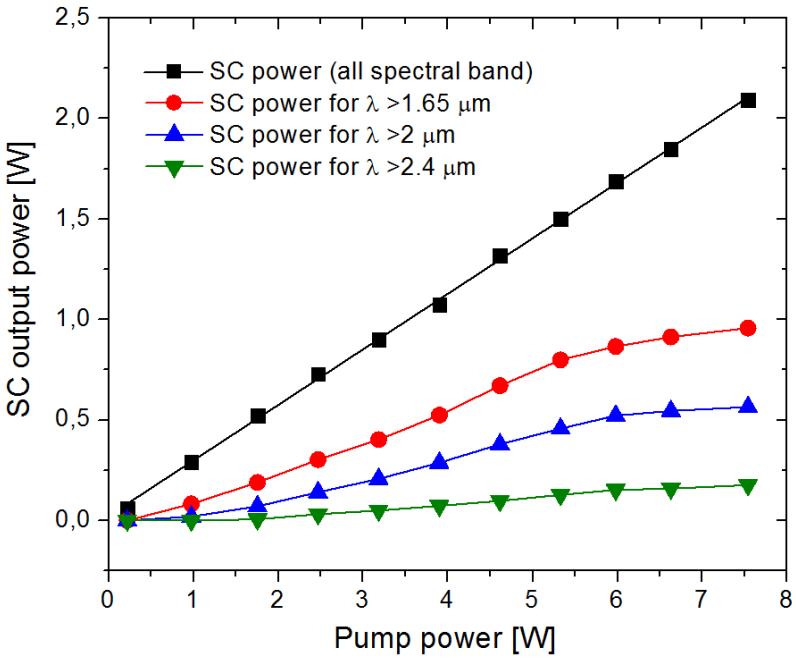

Figure 4-28: SC Average Output Power vs. Launched Pump Power, Measured for 1 ns Pulses and 0.42 MHz Repetition Rate.

Figure 4-29 illustrates the output SC spectrum at the fluoride fiber output. The inset shows the ratio of SC output power measured for λ > 1.65 μm to SC power in the whole spectral band versus launched pump power. The spectrum was measured using two optical spectrum analyzers (measurement in the range of 0.6 – 2.4 μm) and a monochromator with a thermoelectrically cooled HgCdTe detector (for wavelength beyond 2.4 μm). The pump signal was first broadened in the 1.5-m long SMF covering the band of 1.45 – 2.15 μm and then it was launched into the fluoride fiber. Since the fluoroindate fiber has the ZDW at 1.83 μm, it was pumped both in normal and anomalous dispersion region. It means that Raman-induced scattering was mainly responsible for the spectrum extension towards the mid-IR while self-phase modulation and dispersive wave generation contribute to spectrum extension towards shorter wavelengths [39],[40]. As can be seen, the output spectrum spreads from ~ 1 μm to 3.05 μm with a residual peak at the pump wavelength. The 10 dB flatness, excluding the pump peak, is kept in the range of ~ 1.2 – 2.4 μm. For wavelengths longer than 2.4 μm the output signal slowly drops, which results mainly from the fiber attenuation. Further spectral extension could be possible by decreasing the PRF. However the current pump system at lower frequencies (< 400 kHz) reveals significant growth of the 1 μm ASE in the power erbium:ytterbium amplifier. The build-up of the ASE may arise from the high ytterbium doping concentration of the LMA Yb^{+3}-doped fiber, manifesting itself at low duty factors. As Figure 4-29 illustrates, at the short-wavelength part of the spectrum, the ASE signal at about 1.06 μm is clearly visible.

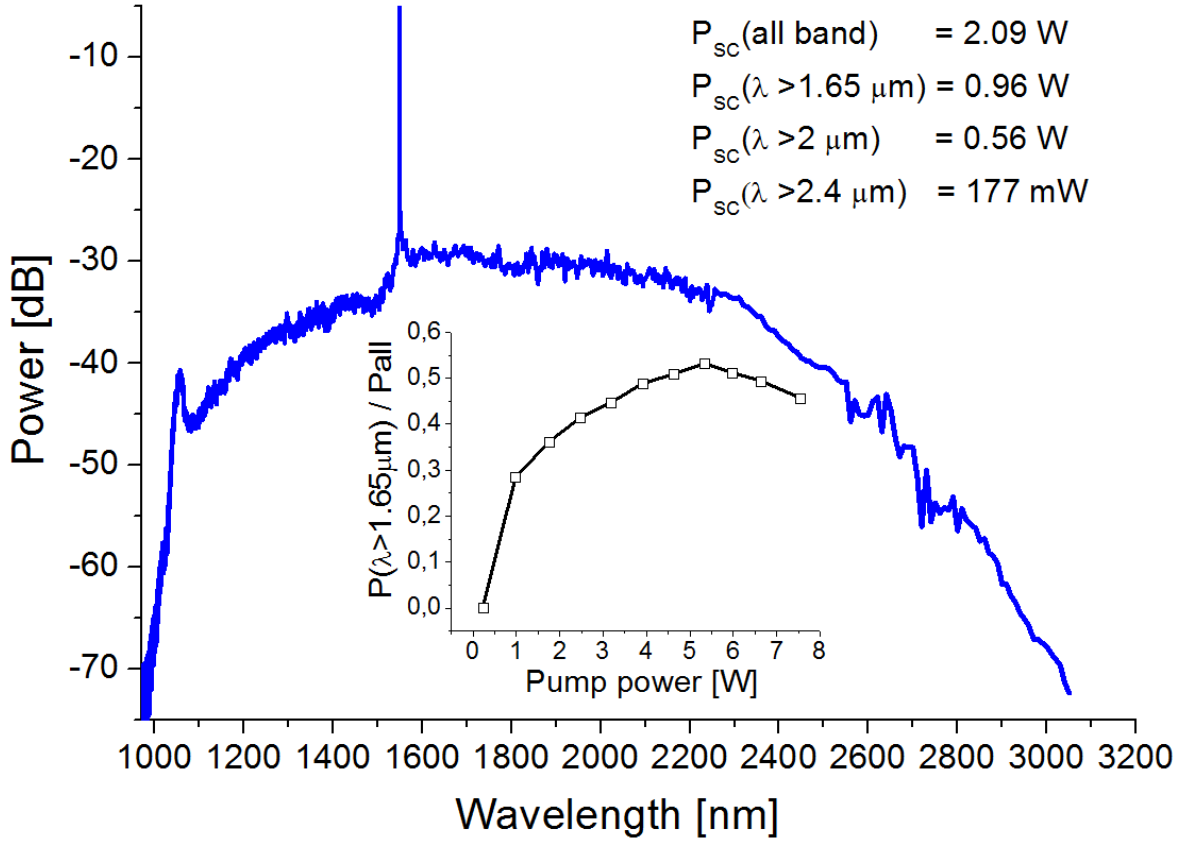

Figure 4-29: SC Spectrum after Propagation Through the Fluoroindate Fiber for the Maximum Output Power. Inset, the ratio of SC output power measured for λ > 1.65 μm to SC power in the whole spectral band versus launched pump power.

Another feature of the observed SC generation is that there was a pump power level, at which spectral broadening towards longer wavelengths was ineffective. As can be seen in the inset in Figure 4-29, for pump power > 5.3 W the ratio of SC power at λ > 1.65 μm to SC in the whole recorded spectral band started to

drop and the power was distributed more effectively towards shorter wavelengths. As Figure 4-28 illustrates, the SC power measured in the whole spectral band increases linearly with the increase in pump power reaching 27% of slope efficiency. However, in case of SC power measured for $\lambda > 1.65$ μm, the slope efficiency is 15.7% (for pump power up to 5.3 W) and then with further increase in pump power it falls to 7.1%. We believe that such behaviour is caused by more effective conversion to a shorter wavelength range, probably due to pumping the fluoroindate fiber more intensively in the normal dispersion region.

The measured spectrum covers over 2000 nm span and it could be further extended by applying more powerful pump source and by using an indium fluoride fiber with smaller core. The fiber non-linearity is defined by the non-linear parameter $\gamma = 2\pi n_2/\lambda A_{eff}$, where n_2 is the non-linear refractive index, λ is the wavelength of the pump pulse and A_{eff} is the effective mode area of a mode propagating inside the fiber. It means that the effective mode area and thus fiber core directly affects the fiber non-linearity. In our case the fluoroindate fiber has the core diameter of 16.7 μm, which is large comparing, e.g. with ZBLAN fibers, where a core diameter is ~ 7 μm, allowing for efficient SC generation even beyond 4.4 μm [23]. The fiber attenuation could be also reduced leading to more effective non-linear interaction and lower thermal load.

In conclusion, the first demonstration of high average power SC generation in a 8-m long step-index indium fluoride fiber pumped by a 1.55 μm MOPA system is reported. A SC extending from 1 μm to 3.05 μm with 2.09 W of total average output power was demonstrated. The system was tested over a week for several hours per day and any fiber degradation was not noticed. The output power of the system should be further scaled up by applying more pump power, lowering the PRF and using a fluoroindate fiber with lower material losses. It should also provide more efficient SC spectrum extension.

4.3 CONCLUSIONS

Mid-Infrared (MIR) Supercontinuum (SC) generation has attracted great attention from the research community, mainly due to its numerous potential applications in infrared microscopy, spectroscopy, medicine, and military technique. Most of the applications require high power, broadband sources emitting radiation in the 2 – 5 μm spectral band. Up to now, there have been many reports on mid-infrared SC generation in soft-glass fibers, including telluride, chalcogenide, and fluoride fibers pumped by a variety of laser sources. However, most of the reported works concern experiments with high peak power femtosecond lasers or optical parametric amplifiers, where output average pump power and thus output SC power is limited to mW-level. To achieve high average power, longer pump pulses on the picosecond or nanosecond scale are needed. Sparse literature reports on high-power (> 0.5 W) SC generation show that this technology is still in its infancy. However, the latest results, including the ones reported by the NATO SET-170 RTG, indicate that the objective of developing ruggedized, ready-to-use, multi-watt supercontinuum sources should be met in the near future.

The highlights of the research on mid-IR SC generation carried out by the members of NATO SET-170 RTG are as follows:

- The first demonstration of the highest average SC power (0.565 W) and the broadest spectrum (1.9 – 4.8 μm) directly emitted from a step-index chalcogenide (As_2S_3) fiber.
- The first demonstration of broadband (2.7 – 4.7 μm) mid-IR SC generation in a step-index indium fluoride (fluoroindate) fiber.
- The first demonstration of Watt-level (2.09 W in the 1 – 3.05 μm spectral band) SC generation in a step-index indium fluoride (fluoroindate) fiber.
- The first demonstration of Watt-level (1.08 W) SC generation (from 1.9 μm to 3.6 μm) in a ZBLAN fiber pumped by an actively Q-switched and mode-locked Tm-doped fiber laser (the pump laser is an example of single pump oscillator approach, making this pump scheme promising for future high power SC sources).

- The first demonstration of Watt-level (1.25 W in the 1.8 – 4.15 μm spectral band) SC generation in a step-index ZBLAN fiber pumped by a fast gain-switched Tm-doped fiber laser and amplifier system.
- The first demonstration of most efficient SC power distribution towards the mid-IR (from 288 mW of output power, 266 mW (92%), 240 mW (83%), 167 mW (58%) and 60 mW (21%) were measured for wavelengths beyond 2 μm, 2.4 μm, 3 μm and 3.6 μm, respectively).

Analyzing the foregoing results as well as the results presented in the available literature recently it can be stated that practical realization of broadband, high average power mid-IR supercontinuum sources that could meet requirements imposed by many applications (especially military applications) is still challenging. This challenge concerns both non-linear media suitable for mid-IR SC generation as well as pump lasers. The most significant factors that limit the long-wavelength edge of the SC spectrum are fiber non-linearities, bend-induced loss and fiber material absorption. The most promising non-linear fibers are telluride, chalcogenide and fluoride based fibers. The first two groups are characterized by very high non-linearity facilitating efficient spectrum extension over short fiber lengths, however these glasses are susceptible to thermally induced damage at high powers thus limiting the output average power < 2 W. The most perspective fibers for high-power SC generation seem to be fluoride (ZBLAN) fibers, in which 10.5 W of average power (in the 0.8 – 4 μm spectral band) has been reported recently. According to the theoretical analysis [33] the average power of the mid-IR SC generated in a single-mode ZBLAN fiber can be further scaled up to ~ 15 W and even to ~ 40 W by implementing better thermal management and heat dissipation techniques (e.g. wrapping an optical fiber with a thermal pad with high thermal conductivity). The same power limitation could be addressed to fluoroindate fibers, but contrary to ZBLAN fibers they are transparent to ~ 5.5 μm, therefore enabling covering the whole 2 – 5 μm spectral band.

Using novel, reliable and high-power fiber-based laser systems facilitating coupling the pump light into a non-linear fiber, output average power of > 20 W from a single-mode fluoride fiber covering the mid-IR band should be achieved within the next 2 – 5 years.

4.4 REFERENCES

[1] Kudlinski, A., George, A.K., Knight, J.C., Travers, J.C., Rulkov, A.B., Popov, S.V. and Taylor, J.R. Zero-dispersion wavelength decreasing photonic crystal fibers for ultraviolet-extended supercontinuum generation, Opt. Express 14, 5715-22 (2006).

[2] Swiderski, J. and Michalska, M. Mid-infrared supercontinuum generation in a single-mode thulium-doped fiber amplifier, Laser Phys. Lett. 10, 035105 (2013).

[3] Cumberland, B.A., Travers, J.C., Popov, S.V. and Taylor, J.R. 29 W high power CW supercontinuum source, Opt. Express 16, 5954-62 (2008).

[4] Baronio, F., Conforti, M., Angelis, C.D., Modotto, D., Wabnitz, S., Andreana, M., Tonello, A., Leproux, P. and Couderc, V. Second and third order susceptibilities mixing for supercontinuum generation and shaping, Opt. Fiber Technol. 18, 283-9 (2012).

[5] Moller, U., Sorensen, S.T., Larsen, C., Moselund, P.M., Jakobsen, C., Johansen, J., Thomsen, C.L. and Bang, O. Optimum PCF tapers for blue-enhanced supercontinuum sources. Opt. Fiber Technol. 18, 304-314 (2012).

[6] Dudley, J.M., Genty, G. and Coen, S. Supercontinuum generation in photonic crystal fiber, Rev. Modern Phys. 78, 1135-84 (2006).

[7] Izawa, T., Shibata, N. and Takeda, A. Optical attenuation in pure and doped fused silica in their wavelength region, Appl. Phys. Lett. 31, 33-35 (1977).

[8] Liao, M., Gao, W., Duan, Z., Yan, X., Suzuki, T. and Ohishi, Y. Supercontinuum generation in short tellurite microstructured fibers pumped by a quasi-cw laser, Opt. Lett. 37, 2127-29 (2012).

[9] Domachuk, P., Wolchover, N.A., Cronin-Golomb, M., Wang, A., George, A.K., Cordeiro, C.M.B., Knight, J.C. and Omenetto, F.G. Over 4000 nm bandwidth of mid-IR supercontinuum generation in sub-centimeter segments of highly nonlinear tellurite PCFs, Opt. Express 16, 7161-68 (2008).

[10] Ebendorff-Heidepriem, H., Kuan, K., Oermann, M.R., Knight, K. and Monro, T.M. Extruded tellurite glass and fibers with low OH content for mid-infrared applications, Opt. Mat. Express 2, 432-42 (2012).

[11] Gattass, R.R., Shaw, L.B., Nguyen, V.Q., Pureza, P.C., Aggarwal, I.D. and Sanghera, J.S. All-fiber chalcogenide-based mid-infrared supercontinuum source, Opt. Fiber Technol. 18, 345-8 (2012).

[12] Sanghera, J.S., Aggarwal, I.D., Shaw, L.B., Florea, C.M., Pureza, P., Nguyen, V.Q. and Kung, F. Nonlinear properties of chalcogenide glass fibers, J. Optoelectron. Advan. Mat. 8, 2148-55 (2006).

[13] Marandi, A., Rudy, C.W., Plotnichenko, V.G., Dianov, E.M., Vodopyanov, K.L. and Byer, R.L. Mid-infrared supercontinuum generation in tapered chalcogenide fiber for producing octave-spanning frequency comb around 3 μm, Opt. Express 20, 24218-25 (2012).

[14] Eckerle, M., Kieleck, C., Swiderski, J., Jackson, S.D., Mazé, G. and Eichhorn, M. Actively Q-switched and mode-locked Tm^{3+}-doped silicate 2 μm fiber laser for supercontinuum generation in fluoride fiber, Opt. Lett. 37, 512-14 (2012).

[15] Qin, G., Yan, X., Kito, C., Liao, M., Chaudhari, C., Suzuki, T. and Ohishi, Y. Ultrabroadband supercontinuum generation from ultraviolet to 6.28 μm in a fluoride fiber, Appl. Phys. Lett. 95, 161103 (2009).

[16] Alexander, V.V., Kulkarni, O.P., Kumar, M., Xia, C., Islam, M.N., Terry Jr., F.L., Welsh, M.J., Ke, K., Freeman, M.J., Neelakandan, M. and Chan, A. Modulation instability initiated high power all-fiber supercontinuum lasers and their applications, Opt. Fiber Technol. 18, 349-74 (2012).

[17] Buczynski, R., Bookey, H.T., Pysz, D., Stepien, R., Kujawa, I., McCarthy, J.E., Waddie, A.J., Kar, A.K. and Taghizadeh, M.R. Supercontinuum generation up to 2.5 μm in photonic crystal fiber made of lead-bismuth-galate glass, Laser Phys. Lett. 7, 666-72 (2010).

[18] Saad, M. Fluoride glass fiber: state of the art, Proc. SPIE 7316, 73160N-1-16 (2009).

[19] Monro, T.M. and Ebendorff-Heidepriem, H. Progress in microstructured optical fibers, Annual Review of Material Research 36, 467-95 (2006).

[20] Hu, J., Menyuk, C.R., Shaw, L.B., Sanghera, J.S. and Aggarwal, I.D. Computational study of 3–5 μm source created by using supercontinuum generation in As2S3 chalcogenide fibers with a pump at 2 μm, Opt. Lett. 35, 2907-2909 (2010).

[21] Hu, J., Menyuk, C.R., Shaw, L.B., Sanghera, J.S. and Aggarwal, I.D. Maximizing the bandwidth of supercontinuum generation in As2Se3 chalcogenide fibers, Opt. Express 18, 6722-6739 (2010).

[22] Xia, C., Kumar, M., Kulkarni, O.P., Islam, M.N., Terry Jr., F.L., Freeman, M.J., Poulain, M. and Mazé, G. Mid-infrared supercontinuum generation to 4.5 μm in ZBLAN fluoride fibers by nanosecond diode pumping, Opt. Lett. 31, 2553-2555 (2006).

[23] Kulkarni, O.P., Alexander, V.V., Kumar, M., Freeman, M.J., Islam, M.N., Terry, J., Neelakandan, M. and Chan, A. Supercontinuum generation from 1.9 to 4.5 μm ZBLAN fiber with high average power generation beyond 3.8 μm using a thulium doped fiber amplifier, J. Opt. Soc. Am. B 28, 2486-2498 (2011).

[24] Gao, W., Amraoui, M.E., Liao, M., Kawashima, H., Duan, Z., Deng, D., Cheng, T., Suzuki, T., Messaddeq, Y. and Ohishi, Y. Mid-infrared supercontinuum generation in a suspended-core As2S3 chalcogenide microstructured optical fiber, Opt. Exp. 21, 9573-9583 (2013).

[25] Swiderski, J. and Michalska, M. Watt-level, all-fiber supercontinuum source based on telecom-grade fiber components, Appl. Phys. B 109, 177-181 (2012).

[26] Monro, T.M. and Ebendorff-Heidepriem, H. Progress in microstructured optical fibers, Annu. Rev. Mater. Res. 36, 467-495 (2006).

[27] Tolstik, N., Sorokin, E., Kalashnikov, V. and Sorokina, I. Soliton delivery of mid-infrared femtosecond pulses with ZBLAN fiber, Opt. Express 2, 1580-1587 (2012).

[28] Zhu, X. and Peyghambarian, N. High-Power ZBLAN Glass Fiber Lasers: Review and Prospect, Adv. In OptoElect. 2010, 1-23 (2010).

[29] Asobe, M., Suzuki, K., Kanamori, T. and Kubodera, K. Nonlinear refractive index measurement in chalcogenide-glass fibers by self-phase modulation, Appl. Phys. Lett. 60, 1153 (1992).

[30] Sanghera, J.S., Aggarwal, I.D., Shaw, L.B., Florea, C.M., Pureza, P., Nguyen, V.Q., Kung, F. and Aggarwal, I.D. Nonlinear properties of chalcogenide glass fibers, J. Opto-Elect. & Adv. Mat. 8, 2148-2155 (2006).

[31] Gattass, R.R., Shaw, L.B., Nguyen, V.Q., Pureza, P.C., Aggarwal, I.D. and Sanghera, J.S. All-fiber chalcogenide-based mid-infrared supercontinuum source, Opt. Fiber Technol. 18 345-348 (2012).

[32] Xia, C., Kumar, M., Cheng, M.-Y., Hegde, R.S., Islam, M.N., Galvanauskas, A., Winful, H.G. and Terry, Jr., F.L. Power scalable mid-infrared supercontinuum generation in ZBLAN fluoride fibers with up to 1.3 watts time-averaged power, Opt. Express 15, 865-871 (2007).

[33] Xia, C., Xu, Z., Islam, M.N., Terry, Jr., F.L., Freeman, M.J., Zakel, A. and Mauricio, J. 10.5 W Time-Averaged Power Mid-IR Supercontinuum Generation Extending Beyond 4 μm With Direct Pulse Pattern Modulation, IEEE Quantum Elect. 15, 422-434 (2009).

[34] Lamont, M.R.E., Luther-Davies, B., Choi, D.-Y., Madden, S. and Eggleton, B.J. Supercontinuum generation in dispersion engineered highly nonlinear (γ = 10 /W/m) As_2S_3 chalcogenide planar waveguide, Opt. Express 15, 14938-14944 (2008).

[35] Kumar, M., Islam, M.N., Terry, F.L., Freeman, M.J., Chan, A., Neelakandan, M. and Manzur, T. Stand-off detection of solid targets with diffuse reflection spectroscopy using a high-power mid-infrared supercontinuum source, Appl. Opt. 51, 2794-2807 (2012).

[36] Yang, W., Zhang, B., Yin, K., Zhou, X. and Hou, J. High power all fiber mid-IR supercontinuum generation in a ZBLAN fiber pumped by a 2 μm MOPA system, Opt. Express 21, 19732-19742 (2013).

[37] Thapa, R., Rhonehouse, D., Nguyen, D., Yao, Z., Zong, J. and Chavez-Pirson, A. Ultra-wide mid-IR supercontinuum generation in W-type tellurite fiber pumped by 2 micron ultrashort laser, in Frontiers in Optics 2012/Laser Science XXVIII, OSA Technical Digest (Optical Society of America), Paper FW4D.2 (2012).

[38] Dudley, J.M. and Taylor, J.R. Supercontinuum generation in optical fibers (Cambridge University Press, 2010).

[39] Agger, C., Petersen, C., Dupont, S., Steffensen, H., Lyngsøn, J.K., Thomsen, C.L., Thøgersen, J., Keiding, S.R. and Bang, O. Supercontinuum generation in ZBLAN fibers—detailed comparison between measurement and simulation, , J. Opt. Soc. Am. B 29, 635-645 (2012).

[40] Agrawal, G.P. Nonlinear Fiber Optics, 4th Edition (Academic Press, 2007).

[41] Dudley, J.M., Provino, L., Grossard, N., Maillotte, H., Windeler, R.S., Eggleton, B.J. and Coen, S. Supercontinuum generation in air-silica microstructured fibers with nanosecond and femtosecond pulse pumping, J. Opt. Soc. Am. B 19, 765-71 (2002).

[42] Geng, J., Wang, Q. and Jiang, S. High-spectral-flatness mid-infrared supercontinuum generated from a Tm-doped fiber amplifier, Appl. Opt. 51, 834-40 (2012).

[43] Kurkov, A.S., Kamynin, V.A., Sholokhov, E.M. and Marakulin, A.V. Mid-IR supercontinuum generation in Ho-doped fiber amplifier, Laser Phys.Lett. 8, 754-57 (2011).

[44] Pioger, P.H., Couderc, V., Leproux, P. and Champert, P.A. High spectral power density supercontinuum generation in a nonlinear fiber amplifier, Opt. Express 15, 11358-63 (2007).

[45] Akhmediev, N. and Karlsson, M. Cherenkov radiation emitted by solitons in optical fibers, Phys.Rev. A 51, 2602-07 (1995).

[46] Dudley, J.M., Genty, G., Dias, F., Kibler, B. and Akhmediev, N. Modulation instability, Akhmediev breathers and continuous wave supercontinuum generation. Opt. Express 17, 21497-21508 (2009).

[47] Skryabin, D.V. and Yulin, A.V. Theory of generation of new frequencies by mixing of solitons and dispersive waves in optical fibers, Phys. Rev. E 72, 016619 (2005).

[48] Jiang, M. and Tayebati, P. Stable 10 ns, kilowatt peak-power pulse generation from a gain-switched Tm-doped fiber laser, Opt. Lett. 32, 1797-1799 (2007).

[49] Larsen, C., Sorensen, S.T., Noordegraaf, D., Hansen, K.P., Mattsson, K.E. and Bang, O. Zero-dispersion wavelength independent quasi-CW pumped supercontinuum generation, Opt. Commun. 290, 170-174 (2013).

[50] Swiderski, J. and Michalska, M. Generation of self-mode-locked resembling pulses in a fast gain-switched thulium-doped fiber laser, Opt. Lett. 38, 1624-1626 (2013).

[51] Hagen, C.L., Walewski, S.W. and Sanders, S.T. IEEE Photon. Technol. Lett. 18, 91 (2006).

[52] Hübner, P., Kieleck, C., Jackson, S.D. and Eichhorn, M. Opt. Lett. 36, 2483 (2011).

[53] Shaw, L.B., Thielen, P.A., Kung, F.H., Nguyen, V.Q., Sanghera, J.S. and Aggarwal, I.D. IR supercontinuum generation in As–Se photonic crystal fiber, in: Proc. Advanced Solid State Photonics, Paper TuC5 (2005).

[54] Shaw, L.B., Gattass, R.R., Sanghera, J.S. and Aggarwal, I.D. All-fiber mid-IR supercontinuum source from 1.5 to 5 um, in: Proc. SPIE 7914, 7914-24 (2011).

[55] Price, J.H., Monro, T.M., Ebendorff-Heidepriem, H., Poletti, F., Horak, P., Finazzi, V., Leong, J.Y., Petropoulos, P., Flanagan, J.C., Brambilla, G., Feng, X. and Richardson, D.J. Mid-IR supercontinuum generation from nonsilica microstructured optical fibers, IEEE J. Sel. Top. Quant. Electron. 13, 738-749 (2007).

[56] Hagen, C.L., Walewski, J.W. and Sanders, S.T. Generation of a continuum extending to the midinfrared by pumping ZBLAN fiber with an ultrafast 1550-nm source, IEEE Photon. Technol. Lett. 18, 91-93 (2006).

[57] Ta'eed, V., Baker, N.J., Fu, L., Finsterbusch, K., Lamont, M.R.E., Moss, D.J., Nguyen, H.C., Eggleton, B.J., Choi, D.-Y., Madden, S. and Luther-Davies, B. Ultrafast all optical chalcogenide glass photonic circuits, Opt. Express 15, 9205-9221 (2007).

[58] Asobe, M., Kanamori, T., Naganuma, K., Itoh, H. and Kaino, T. Third-order nonlinear spectroscopy in As_2S_3 chalcogenide glass fibers, J. Appl. Phys. 77, 5518-5523 (1995).

[59] Xiong, C., Magi, E., Luan, F., Tuniz, A., Dekker, S., Sanghera, J.S., Shaw, L.B., Aggarwal, I.D. and Eggleton, B.J. Characterization of picosecond pulse nonlinear propagation in chalcogenide As2S3 fiber, Appl. Opt. 48, 5467-5474 (2009).

[60] Fortin, V., Bernier, M., Carrier, J. and Vallée, R., Fluoride glass Raman fiber laser at 2185 lm, Opt. Lett. 36, 4152-4154 (2011).

[61] Sanghera, J.S., Brandon Shaw, L. and Aggarwal, I.D., Chalcogenide glass-fiber-based mid-IR sources and applications, IEEE J. Sel. Top. Quant Electron. 15, 114-119 (2009).

[62] Lou, J.W. and Currie, M. High-energy saturable absorber mode-locked fiber laser system, Opt. Lett. 30, 406-408 (2005).

[63] Imeshev, G. and Fermann, M. 230-kW peak power femtosecond pulses from a high power tunable source based on amplification in Tm-doped fiber, Opt. Express 13, 7424-7431 (2005).

[64] Nguyen, V.Q., Sanghera, J.S., Cole, B., Pureza, P., Kung, F.H. and Aggarwal, I.D. Fabrication of arsenic sulfide optical fiber with low hydrogen impurities, J. Am. Ceram. Soc. 85, 2056-2058 (2002).

[65] Rice, J.P., Brown, S.W. and Neira, J.E. Development of hyperspectral image projectors, Proc. SPIE 6297, 629701 (2006).

[66] Rice, J.P., Neira, J.E., Kehoe, M. and Swanson, R. DMD diffraction measurements to support design of projectors for test and evaluation of multispectral and hyperspectral imaging sensors, Proc. SPIE 7210, 72100D (2009).

[67] Shaw, L.B., Gattass, R.R., Sanghera, J.S., Aggarwal, I.D. and Rice, J.P. Broadband mid-IR fiber supercontinuum source for hyperspectral image projection, in: 2011 IEEE Photonics Society Summer Topical Meeting Series, IEEE, pp. 93-94 (2011).

[68] Tolstik, N., Sorokin, E., Kalashnikov, V. and Sorokina, I. Soliton delivery of mid-infrared femtosecond pulses with ZBLAN fiber, Opt. Express 2, 1580-1587 (2012).

[69] Soufiane, A., Can, F., Helgouach, H.L. and Poulain, M. Material dispersion in optimized fluoroindate glasses, J. Non-Cryst. Sol. 184, 36-39 (1995).

[70] Schmidt, E., Shiner, A.D., Giguère, M., Lassonde, P., Trallero-Herrero, C.A., Kieffer, J.-C., Corkum, P.B., Villeneuve, D.M. and Légaré, F. High harmonic generation with long-wavelength few-cycle laser pulses, J. Phys. B: At. Mol. Opt. Phys. 45, 074008 (2012).

[71] Yan, X., Kito, C., Miyoshi, S., Liao, M., Suzuki, T. and Ohishi, Y. Raman transient response and enhanced soliton self-frequency shift in ZBLAN fiber, J. Opt. Soc. Am. B 29, 238-243 (2012).

[72] Saad, M. Indium fluoride glass fibers, Proc. SPIE 8275, 82750D (2012).

[73] Heidt, M., Li, Z., Sahu, J., Shardlow, P.C., Becker, M., Rothhardt, M., Ibsen, M., Phelan, R., Kelly, B., Alam, S.U. and Richardson, D.J. 100 kW peak power picosecond thulium-doped fiber amplifier system seeded by a gain-switched diode laser at 2 μm, Opt. Lett. 38, 1615-1617 (2013).

[74] Swiderski, J. and Michalska, M. Over three-octave spanning supercontinuum generated in a fluoride fiber pumped by Er&Er:Yb-doped and Tm-doped fiber amplifiers, Opt. & Laser Technol. 52, 75-80 (2013).